A new type of mouse gaze shift is led by directed saccades

Sebastian H. Zahler[1,2,4], David E. Taylor[1,2,4], Joey Y. Wong[1], Julia M. Adams[1], and Evan H. Feinberg[1,2,3,*]

1. Department of Anatomy, University of California, San Francisco, San Francisco, CA 94158
2. Neuroscience Graduate Program, University of California, San Francisco, San Francisco, CA 94158
3. Kavli Institute for Fundamental Neuroscience, University of California, San Francisco, San Francisco, CA 94158
4. These authors contributed equally
*Corresponding author: evan.feinberg@ucsf.edu

Abstract:

Animals investigate their environments by directing their gaze towards salient stimuli. In the prevailing view, mouse gaze shifts are led by head rotations that trigger compensatory, brainstem-mediated eye movements, including saccades to reset the eyes. These "recentering" saccades are attributed to head movement-related vestibular and optokinetic cues. However, microstimulating mouse superior colliculus (SC) elicits directed head and eye movements that resemble SC-dependent sensory-guided gaze shifts made by other species, raising the possibility mice generate additional types of gaze shifts. We investigated this possibility by tracking eye and attempted head movements in a head-fixed preparation that eliminates head movement-related sensory cues. We found tactile stimuli evoke gaze shifts involving directed saccades that precede attempted head rotations. Optogenetic perturbations revealed SC drives touch-evoked gaze shifts. Thus, mice make sensory-guided, SC-dependent gaze shifts led by directed saccades. Our findings uncover diversity in mouse gaze shifts and provide a foundation for studying head-eye coupling.

Introduction:

Natural environments are complex and dynamic, and animals frequently redirect their gaze to scrutinize salient sensory stimuli. Gaze shifts employ head and eye movement coupling

1 strategies that depend on context and can vary between species (Goldring et al., 1996; Land,

2 2019; Land and Nilsson, 2012; Populin, 2006; Populin and Rajala, 2011; Populin et al., 2004a;

3 Ruhland et al., 2013; Tollin et al., 2005). Mice are an increasingly important model organism in

4 vision research, yet the strategies they use to shift their gaze remain incompletely understood.

5 Revealing these strategies is essential to understanding mouse visual ethology and the

6 underlying neural mechanisms.

7

8 The prevailing view holds that species such as mice whose retinae lack high-acuity

9 specializations (afoveates) generate gaze shifts driven by head movements followed by

10 "recentering" saccades (Land and Nilsson, 2012). Indeed, recent studies tracking head and eye

11 movements in freely moving mice found that spontaneous and visually evoked mouse gaze

12 shifts matched this description (Meyer et al., 2018, 2020; Michaiel et al., 2020; Payne and

13 Raymond, 2017). Specifically, during a gaze shift, slow eye movements stabilize the retinal

14 image by countering the rotation of the head and are punctuated by fast saccadic eye

15 movements to recenter the eyes in the orbits as they approach the end of their range of motion.

16 These recentering saccades—also known as "compensatory" saccades or the quick phase of

17 nystagmus—are centripetal, occur in the direction of the head movement, and are thought to be

18 driven by vestibular or optokinetic signals acting on circuits in brainstem (Curthoys, 2002; Hepp

19 et al., 1993; Kitama et al., 1995; Meyer et al., 2020; Michaiel et al., 2020; Payne and Raymond,

20 2017). These recent observations have buttressed the view that gaze shifts in mice and other

21 afoveates are led by head movements, with eye movements made only to compensate for the

22 effects of head movements. In contrast, primates and other foveate species are capable of an

23 additional form of gaze shift led by directed saccades, with or without directed head movements,

24 to redirect their gaze towards salient stimuli (Bizzi et al., 1972; Freedman, 2008; Lee, 1999;

25 Zangemeister and Stark, 1982). Directed saccades differ from recentering saccades in that they

26 have endpoints specified by the location of the stimulus (and therefore are often centrifugally

2

1   directed), typically occur simultaneously with or slightly before (20-40 ms) head movements

2   during gaze shifts, and are driven by midbrain circuits, particularly the superior colliculus (SC).

3   To date, there is no behavioral evidence that mice or any afoveate species generate directed

4   saccades or gaze shifts led by eye movements.

5

6   However, three observations are inconsistent with the model that all saccades in mice are

7   exclusively recentering and made to compensate for head movements. First, mouse saccades

8   are not only a product of vestibular or optokinetic cues, because head-fixed mice, in which these

9   signals do not occur, generate saccades, albeit less frequently. Second, neuroanatomical and

10   functional studies suggest that the circuits that underlie directed saccades are conserved in

11   mice (May, 2006; Sparks, 1986, 2002). Specifically, microstimulation of the mouse superior

12   colliculus (SC) showed that it contains a topographic map of saccade and head movement

13   direction and amplitude (Masullo et al., 2019; Wang et al., 2015) roughly aligned with maps of

14   visual, auditory, and somatosensory space (Drager and Hubel, 1975, 1976). These SC sensory

15   and motor maps resemble those believed to underlie primates' and cats' ability to make gaze

16   shifts led by directed saccades towards stimuli of these modalities (Sparks, 1986, 2002). Third,

17   saccade-like eye movements occurring in the absence of head movements have occasionally

18   been observed in freely moving mice, albeit infrequently and usually in close proximity to head

19   movements (Meyer et al., 2018, 2020; Michaiel et al., 2020).

20

21   We therefore hypothesized that mice innately generate gaze shifts that incorporate directed

22   saccades. We predicted that this ability was obscured in previous studies for several reasons.

23   First, in freely moving mice it is difficult to uncouple the contributions of reafferent vestibular and

24   optokinetic inputs from those of exafferent (extrinsic) sensory inputs to saccade generation.

25   Second, previous analyses in mice were mostly confined to spontaneous or visually guided

26   gaze shifts, and there is evidence in humans, non-human primates, and cats that gaze shifts in

3

1   response to different sensory modalities can involve distinct head-eye coupling strategies

2   (Goldring et al., 1996; Populin, 2006; Populin and Rajala, 2011; Populin et al., 2004a; Ruhland

3   et al., 2013; Tollin et al., 2005). Third, in freely moving mice it is difficult to present stimuli in

4   specific craniotopic locations. We therefore reasoned that by using a head-fixed preparation

5   both to eliminate vestibular and optokinetic cues and to present stimuli of different modalities at

6   precise craniotopic locations, we could systematically determine whether mice are capable of

7   gaze shifts involving saccades whose endpoints depend on stimulus location and show different

8   coupling to head movements. We found that tactile stimuli evoke saccades whose endpoints

9   depend on stimulus location, that these saccades precede attempted head rotations, and that

10 these touch-evoked gaze shifts are SC-dependent. Together, these results resolve an apparent

11 discrepancy between mouse neuroanatomy and behavior, demonstrating that mice are capable

12 of generating gaze shifts led by directed saccades.

13

14 **Results:**

15 **Stimulus-evoked gaze shifts in head-restrained mice**

16 To test the hypothesis that mice possess an innate ability to make sensory-evoked gaze shifts

17 that incorporate directed saccades coupled to head movements, we head-fixed naïve, wild-type

18 adult animals and used infrared cameras to track both pupils and a strain gauge (also known as

19 a load cell) to measure attempted head rotations. Previous studies in head-fixed mice observed

20 occasional undirected saccades in response to changes in the visual environment (Samonds et

21 al., 2018) and visually guided saccades only after weeks of training and at long (~1 s) latencies

22 (Itokazu et al., 2018). We therefore tested a panel of stimuli of different modalities to determine

23 whether they could evoke saccades. We began by testing the following stimuli from a constant

24 azimuthal location: 1) a multisensory airpuff that provides tactile input to the ears and generates

25 a loud, broadband sound; 2) an auditory stimulus consisting of the same airpuff moved away

26 from the animal so as not to provide tactile input; 3) a tactile stimulus consisting of a bar that

4

1   nearly silently taps the ear; and 4) a visual stimulus consisting of a bright LED. Stimuli were

2   delivered on either side of the animal every 7-12 s in a pseudorandom sequence (Fig. 1A). The

3   probability of horizontal eye movements increased sharply and significantly above the low

4   baseline level (1.3 ± 0.2%, mean ± s.d.) in the 100 ms period following delivery of multisensory

5   airpuffs (ear airpuff: 29.0 ± 7.5%, $p < 0.001$ paired Student's t-test; whisker airpuff: 12.5 ± 2.3%,

6    $p < 0.001$), auditory airpuffs (3.5 ± 1.2%, $p < 0.05$), and tactile stimuli (4.5 ± 0.5%, $p < 0.001$)

7   and remained slightly elevated for at least 500 ms (Fig. 1C-F, H-K; Supplementary Figure 2). In

8   contrast, the probability of saccade generation was not changed by visual stimuli (Fig. 1G, L; 1.3

9   ± 0.2%, $p = 0.61$). We consider these stimulus-evoked eye movements to be saccades because

10   they reached velocities of several hundred degrees per second (Supplementary Fig. 1),

11   displayed a main sequence, *i.e.*, peak velocity scaled linearly with amplitude (Supplementary

12   Fig. 1), and were bilaterally conjugate (Supplementary Fig. 1) (Bahill et al., 1975). As in

13   previous studies, saccade size for temporal-to-nasal movements was slightly larger than for

14   nasal-to-temporal movements (Meyer et al., 2018), but this asymmetry was eliminated by

15   averaging the positions of both pupils (before averaging: temporal saccade amplitude = 10.9 ±

16   0.8° (mean ± s.d.), nasal saccade amplitude = 8.4 ± 1.1°, $p = 0.0009$; after averaging, leftward

17   amplitude = 10.2 ± 1.0°, rightward amplitude = 9.3 ± 0.4°, $p = 0.0986$). We next examined

18   attempted head movements. The baseline frequency of attempted head movements was much

19   higher than that of eye movements (27.8 ± 4.8%, mean ± s.d.). Mirroring results for saccades,

20   auditory, tactile, and audiotactile stimuli evoked attempted head movements but visual stimuli

21   did not (Fig. 1M-Q; auditory: 53.2 ± 21.9%, $p = 0.045$; tactile: 67.1 ± 10%, $p < 0.01$; ear airpuff:

22   86.6 ± 8.7%, $p < 10^{-5}$; whisker airpuff: 79.2 ± 9.5%, $p < 0.001$; visual: 26.9 ± 2.0%, $p = 0.0505$,

23   paired Student's t-test). These data demonstrate that both auditory and tactile stimuli are

24   sufficient to evoke gaze shifts in head-fixed mice, and that mice make sensory-evoked

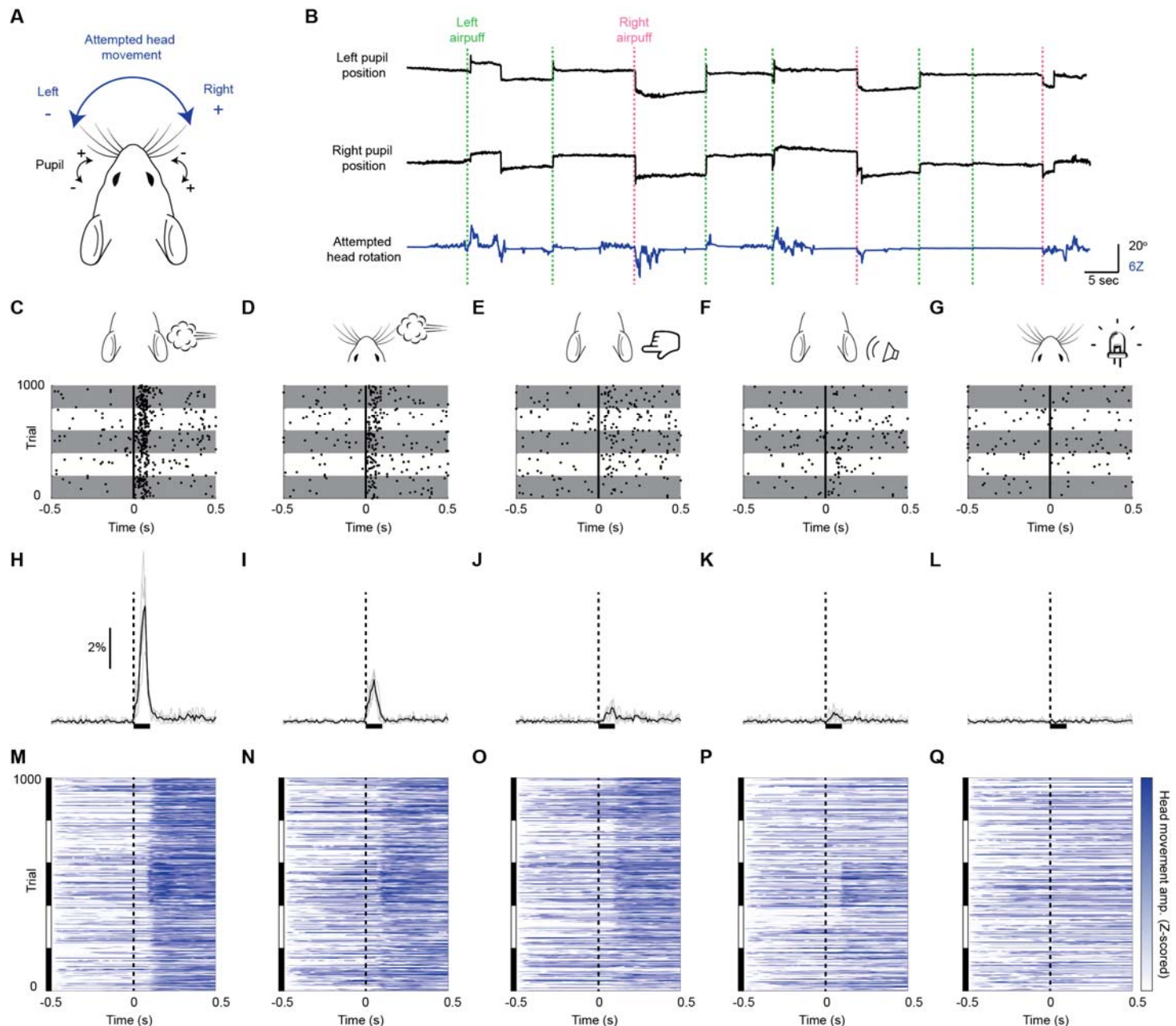25   saccades in the absence of vestibular and optokinetic inputs.

5

1

2 **Figure 1. Mice innately make sound- and touch-evoked gaze shifts. (A)** Behavioral schematic. Naïve mice are

3 head-fixed and stimuli are presented on either side. Both eyes are tracked using cameras and attempted head

4 rotations are measured using a strain gauge (load cell). In subsequent quantification, eye positions to the right of

5 center (nasal for left eye, temporal for right eye) are positive, and eye positions to the left of center (temporal for left

6 eye, nasal for right eye) are negative, with zero defined as the mean eye position. Likewise, attempted rightward

7 head movements are positive, and leftward head movements are negative. **(B)** Sample eye and attempted head

8 movement traces. Dashed vertical lines indicate left (magenta) and right (green) ear airpuff delivery. **(C-G)** Saccade

6

1   rasters for 5 representative mice in response to (C) ear airpuffs, (D) whisker airpuffs, (E) ear tactile stimuli, (F)

2   auditory airpuffs, and (G) visual stimuli. Each row corresponds to a trial. Each dot indicates onset of a saccade.

3   Vertical black lines denote time of left or right stimulus delivery. Each gray or white horizontal stripe contains data for

4   a different mouse. n = 1000 randomly selected trials (200/mouse). **(H-L)** Peri-stimulus time histograms showing

5   instantaneous saccade probabilities in response to (H) ear airpuffs, (I) whisker airpuffs, (J) ear tactile stimuli, (K)

6   auditory airpuffs, and (L) visual stimuli for mice from (C-G). Each light trace denotes a single animal; black traces

7   denote population mean. Dashed lines denote time of stimulus delivery. Horizontal bar indicates the 100 ms response

8   window used in subsequent analyses. **(M-N)** Heatmaps of attempted head movements in response to (M) ear

9   airpuffs, (N) whisker airpuffs, (O) ear tactile stimuli, (P) auditory airpuffs, and (Q) visual stimuli for mice from (C-L).

10   Each row corresponds to an individual trial from C-G. Black and white bars at left indicate blocks of trials

11   corresponding to each of 5 different mice. Dashed line denotes stimulus delivery time.

12

13   **Tactile stimuli evoke directed saccades whose endpoints depend on stimulus location**

14   To determine whether sensory-evoked saccades are directed, we asked whether saccade

15   endpoints are dependent on stimulus location. We began by examining the endpoints of

16   saccades evoked by left and right ear airpuffs (Fig. 2A). We found that left ear airpuffs evoked

17   saccades with endpoints far left of center (with center defined as the mean eye position),

18   whereas right ear airpuffs evoked saccades with endpoints far right of center (left: -5.4 ± 4.5°,

19   right: 5.4 ± 3.4°, mean ± s.d., p < 10^{-10} Welch's t-test, n = 2155 trials). To understand how this

20   endpoint segregation arises, we examined the trajectories of individual saccades (Fig. 2E). We

21   found that left ear airpuffs elicited nearly exclusively leftward saccades (94.2 ± 3.1%, mean ±

22   s.d., n = 5 mice), whereas right ear airpuffs elicited nearly exclusively rightward saccades (96.0

23   ± 2.1%)—often from the same eye positions. By definition, from any eye position, one of these

24   directions must lead away from center and is thus centrifugal rather than centripetal. In addition,

25   puff-evoked saccades that began towards the center often reached endpoints at eccentricities of

26   5 to 10 degrees. To further test whether saccade endpoints are specified by stimulus location,

27   we repositioned the airpuff nozzles to stimulate the whiskers and repeated the experiments. We

28   reasoned that saccade endpoints should become less eccentric as stimulus eccentricity

7

1   decreases. Indeed, airpuffs applied to the whiskers evoked saccades with endpoints central to

2   those evoked by ear airpuff stimulation, such that the ordering of saccade endpoints mirrored

3   that of stimulus locations (Mean endpoints: left ear, -5.4 ± 4.5°; left whiskers, -0.4 ± 3.8°; right

4   whiskers, 0.8 ± 3.9°; right ear, 5.4 ± 3.4°; mean ± s.d., $p < 0.05$ for all pairwise comparisons,

5   paired two-tailed Student's t-test) (Fig. 2A,B; Supplementary Fig. 3). In this cohort, the

6   separation between whisker-evoked saccade endpoints, although significant, was small, but in

7   other cohorts we have observed larger separation (as well as higher auditory-evoked saccade

8   probabilities) (Supplementary Fig. 4). Taken together, these data suggest that touch-evoked

9   saccades are directed towards particular eye positions that are specified by stimulus location.
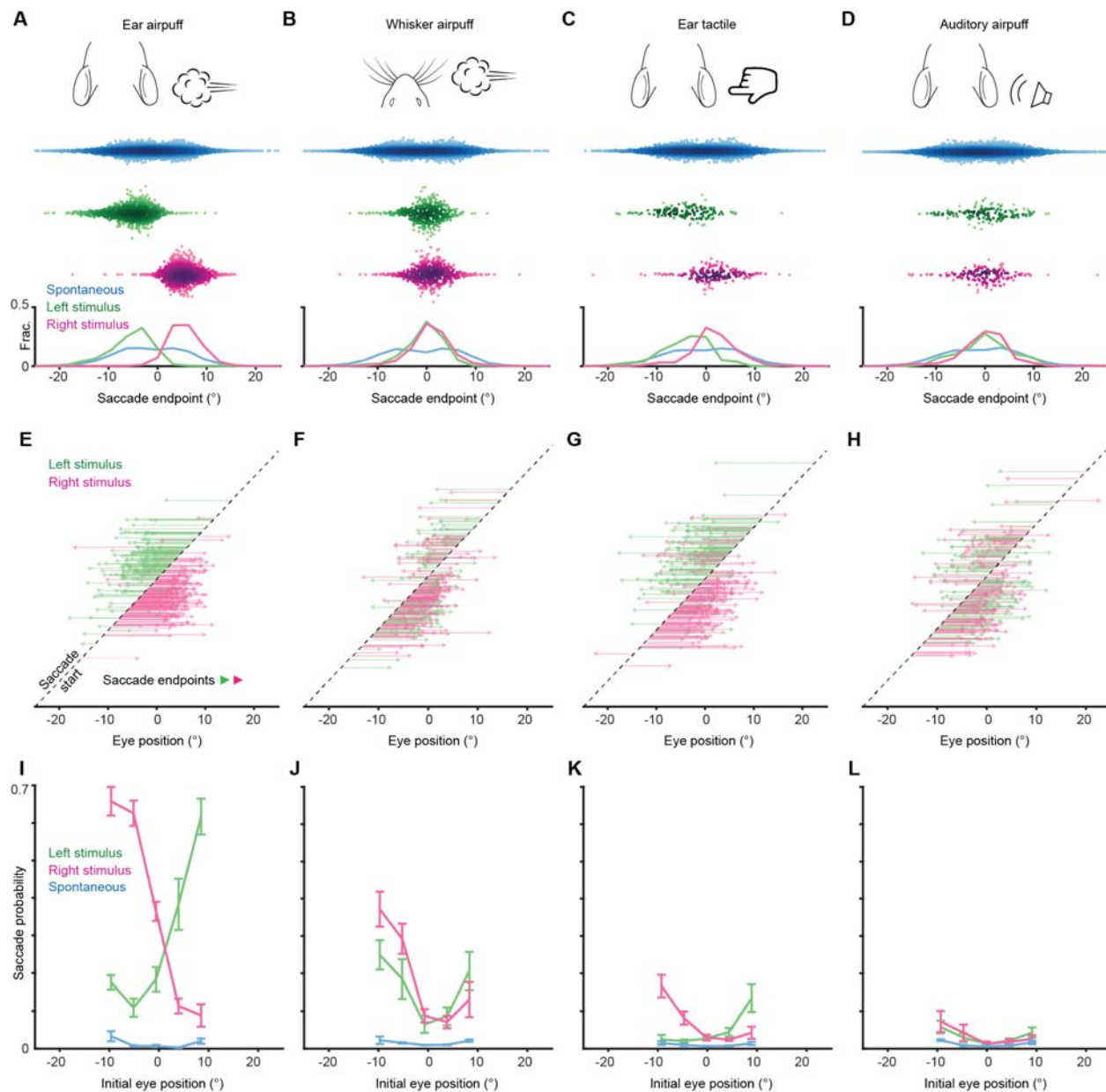
Figure 2. Endpoints and trajectories of sensory-evoked saccades. (A-D) Endpoints for ear airpuff-, whisker airpuff-, ear tactile-, and auditory airpuff-evoked saccade. Top, schematics of stimuli. Middle, scatter plots showing endpoints of all saccades for all animals (n=see below, 5 animals) made spontaneously (blue) and in response to left (green) and right (magenta) stimuli. Darker shading indicates areas of higher density. Bottom, histograms of endpoint distributions for spontaneous and evoked saccades. **(E-H)** Trajectories of individual stimulus-evoked saccades. Each arrow denotes the trajectory of a single saccade. Saccades are sorted according to initial eye positions, which fall on the dashed diagonal line. Saccade endpoints are indicated by arrowheads. Because the probability of evoked gaze shifts differed across stimuli, data for ear and whisker airpuffs are randomly subsampled (15% and 30% of total trials,

9

1   respectively) to show roughly equal numbers of trials for each condition. **(I-L)** Relationship between eye position and

2   saccade probability. Green and magenta lines indicate population means (n = 5 mice) for saccades evoked by left

3   and right stimuli, respectively. Blue lines indicate spontaneous saccades. Error bars indicate s.e.m. Saccade

4   numbers in A-H: ear airpuff sessions, spontaneous = 7146, left ear airpuff-evoked = 942 (141 in E), right ear airpuff-

5   evoked = 1213 (182 in E); whisker airpuff sessions: spontaneous = 7790, left whisker airpuff-evoked = 440 (132 in F),

6   right whisker airpuff-evoked = 606 (181 in F); ear tactile sessions, spontaneous = 6706, left ear tactile-evoked = 133,

7   right ear tactile-evoked = 186; auditory sessions, spontaneous = 10240, left auditory-evoked = 140, right auditory-

8   evoked = 158.

9

10   We next examined the endpoints of saccades evoked by tactile and auditory stimuli. Similar to

11   the multisensory airpuff stimuli, tactile stimuli delivered to the left and right ears evoked

12   saccades whose endpoints were significantly different (-3.9 ± 5.3° (left) vs. 1.5 ± 5.0° (right);

13   mean ± s.d., $p < 10^{-10}$, Welch's t-test, n = 452 trials) and whose directions were largely opposite

14   from nearly all eye positions (left stimuli evoked 77.5 ± 23.7% leftward saccades, right stimuli

15   evoked 78.3 ± 11.6% rightward saccades, n = 5 mice). This result suggests that tactile stimuli

16   are sufficient to induce gaze shifts that involve directed saccades. We next examined the

17   endpoints and trajectories of saccades evoked by left and right auditory stimuli (Fig. 2D, H).

18   Strikingly, the saccade endpoint locations did not differ significantly for left and right auditory

19   stimuli and were located centrally (0.1 ± 5.1° (left) vs. -0.1 ± 5.1° (right); mean ± s.d., p = 0.72,

20   Welch's t-test, n = 298 trials). Because we had fewer trials with sound-evoked gaze shifts

21   overall, to confirm that this lack of statistically significant endpoint separation was not a result of

22   lower statistical power, we repeated our analyses on matched numbers of sound- and touch-

23   evoked saccades sampled at random, once again observing that left and right ear airpuff-,

24   whisker airpuff-, and ear tactile-evoked saccade endpoints were significantly different (ear

25   airpuff, $p < 10^{-10}$; whisker airpuff, p = 0.0039; ear tactile, $p < 10^{-10}$; auditory airpuff, p = 0.50;

26   Welch's t-test, see figure for complete statistics). The central endpoints of sound-evoked

27   saccades arose because, in contrast to touch-evoked saccades, saccades evoked by both right

1 and left stimuli traveled in the same, centripetal direction from all initial eye positions: rightward

2 from eye positions to the left of center, and leftward from eye positions to the right of center

3 (fraction centripetal: left airpuff for initial eye positions left of center, 0.89 ± 0.08; left airpuff for

4 initial eye positions right of center, 0.90 ± 0.09; right airpuff for initial eye positions left of center,

5 0.87 ± 0.07; right airpuff with initial eye positions right of center, 0.76 ± 0.12).. We compared the

6 mean sound-evoked saccade endpoint location to the mean overall eye position and found no

7 significant difference, suggesting that auditory saccades function to recenter ($p = 0.93$, one-

8 sample Student's t-test) (Land and Nilsson, 2012; Meyer et al., 2018, 2020; Michaiel et al.,

9 2020; Paré and Munoz, 2001; Tatler, 2007). Thus, both the auditory and tactile components of

10 the airpuff stimuli are sufficient to evoke saccades but only tactile stimulation evokes directed

11 saccades whose endpoints are specified by the site of stimulation.

12

13 **Starting eye position determines saccade probability**

14 We observed that gaze shifts were generated on a subset of trials. We therefore sought to

15 understand factors underlying the probabilistic nature of evoked gaze shifts. We first examined

16 arousal, which modulates many neuronal and behavioral phenomena, by inferring arousal levels

17 from pupil diameter. Surprisingly, saccade probability did not differ between trials with high

18 (dilated pupils) or low (constricted pupils) arousal (Supplementary Fig. 5) (Reimer et al., 2014).

19 Next, we asked whether novelty plays a role by examining the effects of sensory history.

20 Saccade probability was constant within sessions but declined somewhat over successive

21 sessions, suggesting that sensory history plays a role on long time scales (Supplementary Fig.

22 5). We then examined starting eye position. Strikingly, saccade probability varied strongly with

23 initial eye position (Fig. 2I-L, Supplementary Fig. 4I-L). In addition, the relationship between

24 initial eye position and saccade probability differed across stimuli, with the lowest probability

25 coinciding with the mean endpoint of saccades evoked by that stimulus (Fig. 2A-D, I-L).

26

1   **Stimulus-evoked gaze shifts involve a different type of head-eye coupling**

2   Next, we examined the relationship between attempted head rotations and saccades during

3   gaze shifts. We first analyzed the relative timing of the head and eye components of

4   spontaneous gaze shifts. Previous studies in freely moving and head-fixed mice found that on

5   average, spontaneous and visually evoked saccades in freely moving mice are preceded by

6   head rotations, and that spontaneous saccades in head-fixed mice are similarly preceded by

7   attempted head rotations (Meyer et al., 2018, 2020; Michaiel et al., 2020; Payne and Raymond,

8   2017). Consistent with these observations, we found that on average spontaneous saccades

9   were preceded by attempted head rotations (Fig. 3B, E). Interestingly, attempted head rotations

10 during spontaneous saccades appeared biphasic, with a slower phase beginning before

11 saccades (median: 90 ms before saccade onset) followed by a fast phase beginning slightly

12 after saccade onset. This biphasic response closely resembles the eye-head coupling pattern

13 reported in freely moving mice (Meyer et al., 2020).
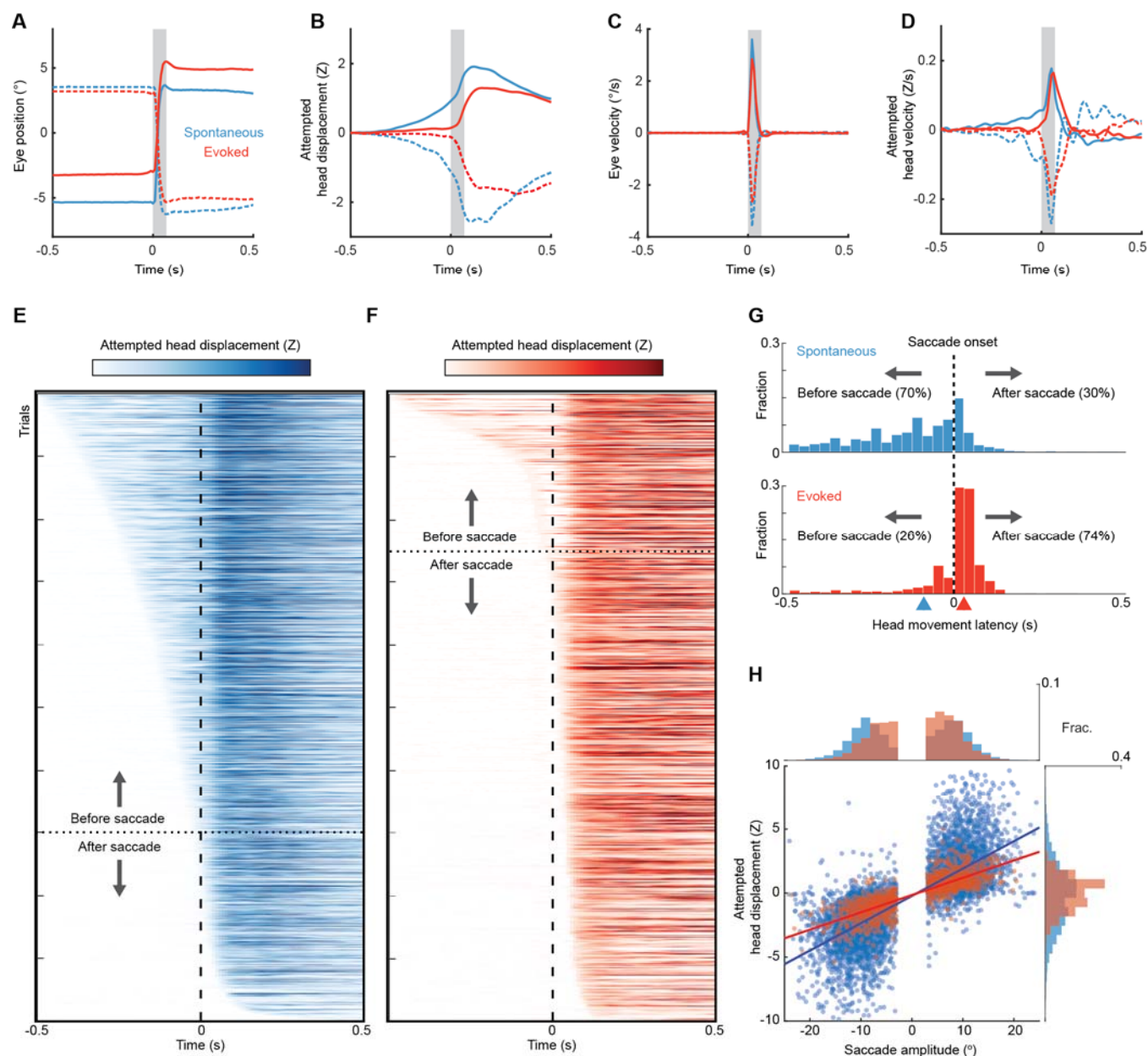
14

Figure 3. Different head-eye coupling during spontaneous and touch-evoked gaze shifts. (A) Mean trajectories

of all rightward (solid traces) and leftward (dashed traces) saccades during spontaneous (blue, n= 7146) and ear

airpuff-evoked (red, n = 1437) gaze shifts. Means + s.e.m. (smaller than line width). Gray bar indicates average

saccade duration. **(B)** Mean attempted head movement amplitudes accompanying rightward (solid traces) and

leftward (dashed traces) saccades during spontaneous (blue) and ear airpuff-evoked (red) gaze shifts. **(C)** Mean

velocities of all rightward (solid traces) and leftward (dashed traces) saccades during spontaneous (blue) and ear

airpuff-evoked (red) gaze shifts. (**D**) Mean attempted head movement velocities accompanying rightward (solid

traces) and leftward (dashed traces) saccades during spontaneous (blue) and ear airpuff-evoked (red) gaze shifts. **(E,**

13

1   **F)** Timing of attempted head movements relative to saccades during all spontaneous (E) and ear airpuff-evoked (F)

2   gaze shifts. Each row corresponds to a single gaze shift. Darker shades indicate larger attempted head displacement.

3   Dashed vertical line indicates time of saccade onset. Trials are sorted according to latency of attempted head

4   movements. Trials above and below dashed horizontal line correspond to attempted head movements that began

5   before and after saccades, respectively. **(G)** Distributions of attempted head movement latencies relative to saccade

6   onset for spontaneous (top) and ear airpuff-evoked (bottom) saccades. Medians indicated by blue and red

7   arrowheads. Distributions are significantly different ($p < 10^{-5}$, permutation test). **(H)** Head-eye amplitude coupling of

8   spontaneous (blue) and ear airpuff-evoked saccades (red). Each dot corresponds to a single gaze shift. Attempted

9   head amplitude was measured 150 ms after saccade onset. Spontaneous: $R^2 = 0.58$, slope = 0.214, $p < 10^{-10}$.

10   Evoked: $R^2 = 0.69$, slope = 0.135, $p < 10^{-10}$. Spontaneous and evoked regression slopes were significantly different (p

11   = 0.01, permutation test). Histograms above and beside scatter plot indicate distributions of saccade and attempted

12   head movement amplitudes, respectively. Mean head and eye movement amplitudes were significantly smaller for

13   airpuff-evoked saccades ($p < 10^{-5}$, permutation test).

14

15   We next asked whether the relative timing of eye and attempted head movements was similar

16   for stimulus-evoked gaze shifts. Surprisingly, ear airpuff-evoked saccades were not preceded by

17   slow attempted head rotations but were nevertheless accompanied by fast attempted head

18   rotations that began slightly after saccade onset (Fig. 3B). This pattern was mirrored in the

19   average eye and attempted head movement traces for whisker airpuff-, auditory airpuff-, and

20   ear tactile-evoked saccades (Supplementary Fig. 6A-D). To better understand how these

21   patterns arose, we examined head and eye movement timing at the single-trial level. For

22   spontaneous gaze shifts, head movement onset fell along a continuum, with the majority of

23   attempted head movements beginning before saccade onset (70%), with a median latency of 90

24   ms before saccade onset (Fig. 3E, G). In contrast, for stimulus-evoked gaze shifts, the vast

25   majority of attempted head movements began after saccade onset (74%), with a median latency

26   of 30 ms after saccade onset (Fig. 3F,G).

27

1   We next examined the amplitudes of head and eye movements during spontaneous and

2   stimulus-evoked gaze shifts. During spontaneous gaze shifts, attempted head rotations were in

3   the same direction as saccades and scaled with saccade amplitude (Fig. 3A, B, H). These data

4   are consistent with eye-head coupling patterns previously observed in both head-fixed and

5   freely moving conditions (Meyer et al., 2020). Similarly, stimulus-evoked gaze shifts involved

6   attempted head rotations that were made in the same direction as saccades and scaled with

7   saccade amplitude (Fig.3A, B, H). Interestingly, stimulus-evoked saccades of a given amplitude

8   were coupled to an average of 37% smaller attempted head movements than were

9   spontaneous saccades, due largely to the lack of slow pre-saccadic head movements observed

10   during spontaneous gaze shifts (linear regression slopes 0.135 vs. 0.214, $p < 10^{-5}$, permutation

11   test). To confirm that the differences in coupling we observed were not an artifact of differences

12   in saccade size and starting position between saccade types, we performed an additional

13   analysis using subsets of gaze shifts matched for saccade amplitude and initial eye position and

14   observed the same effects (Supplementary Fig. 7; linear regression slopes 0.135 vs. 0.224, p <

15   10^{-5}, permutation test).

16

17   Because touch-evoked saccades and attempted head movements are proportional, and our

18   previous analyses showed that saccade direction and amplitude depend on initial eye position

19   (Fig. 2E-H), we asked whether there was a relationship between airpuff-evoked attempted head

20   movements and initial eye position. We analyzed whisker airpuff-evoked gaze shifts because

21   these involved a mixture of saccade directions. Strikingly, both saccade and attempted head

22   movement direction and amplitude were dependent on initial eye position (Supplementary Fig.

23   8).

24

25

26

1   **The superior colliculus mediates airpuff-evoked gaze shifts**

2   We next sought to identify the neural circuitry underlying airpuff-evoked gaze shifts. As

3   discussed previously, in other species, stimulus-evoked gaze shifts involving directed head and

4   eye movements are driven by SC (Freedman, 2008; Freedman et al., 1996; Guitton, 1992;

5   Guitton et al., 1980; Paré et al., 1994). In contrast, it is widely believed that the recentering

6   saccades observed in mice are driven by brainstem circuitry in response to head rotation

7   (Curthoys, 2002; Hepp et al., 1993; Kitama et al., 1995; Meyer et al., 2020; Michaiel et al., 2020;

8   Payne and Raymond, 2017). To determine whether SC is required to generate touch-evoked

9   gaze shifts in mice, we pursued an optogenetic strategy to perturb SC activity in the period

10   surrounding airpuff onset. For inhibition experiments, we stereotaxically injected adeno-

11   associated virus (AAV) encoding the light-gated chloride pump eNpHR3.0 under the control of a

12   pan-neuronal promoter and implanted a fiber optic in right SC (Gradinaru et al., 2010).

13   Consistent with data in foveate species (Hikosaka and Wurtz, 1985; Robinson, 1972; Schiller

14   and Stryker, 1972), optically reducing right SC activity shifted airpuff-evoked saccade endpoints

15   to the right (i.e., ipsilaterally) for both left (-3.7 ± 4.3° (control) vs. -2.3 ± 4.7° (LED on), p <

16   0.001, Welch's t-test) and right ear airpuffs (4.5 ± 4.1° (control) vs. 5.4 ± 4.7° (LED on), p =

17   0.011, Welch's t-test) (Fig. 4A-C). To control for potential mismatches in starting eye position

18   between LED-off and LED-on trials, we performed additional analyses using matched trials and

19   found that the endpoint and amplitude differences persisted (Supplementary Fig. 10). For

20   stimulation experiments, we stereotaxically injected AAV encoding the light-gated ion channel

21   ChR2 under the control of a pan-neuronal promoter and implanted a fiber optic in right SC

22   (Gradinaru et al., 2010). Because strong SC stimulation can evoke saccades, we used weak

23   stimulation (50-120 μW) in order to bias SC activity. This manipulation caused the reciprocal

24   effect of right SC inhibition, biasing endpoints leftwards (*i.e.,* contraversively) for both left (-5.8 ±

25   4.6° (control) vs. -8.0 ± 6.1° (LED on), p = 0.0016, Welch's t-test) and right (5.6 ± 3.5° (control)

26   vs. 1.9 ± 6.1° (LED on), p < 10^{-5}, Welch's t-test) airpuffs (Fig. 4E-G). Once again, controlling for

1   differences in starting eye position between conditions yielded similar results (Supplementary
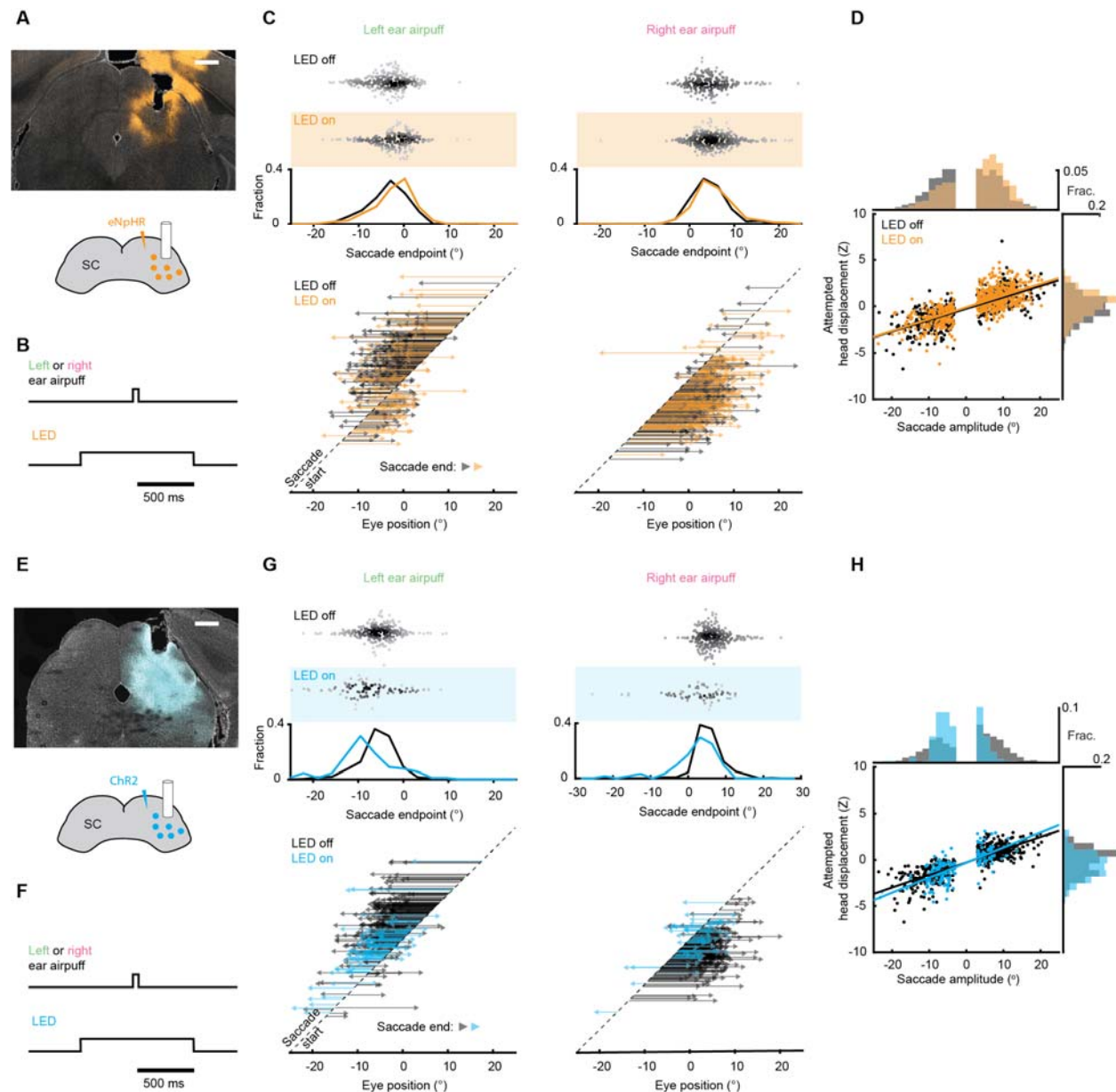
2   Fig. 10).

4   **Figure 4**. **Superior colliculus controls touch-evoke gaze shifts. (A)** Schematic of right SC optogenetic inhibition

5   using eNpHR3.0 and example histology for representative mouse. Scale bar, 0.5 mm. The lack of fluorescence

6   immediately surrounding fiber tip is due to photobleaching by high photostimulation intensity (12 mW, as opposed to

7   50-120 μW for ChR2 experiments in (E-H)). **(B)** Trial structure. Optogenetic illumination is provided for a 1 s period

8   centered around airpuff delivery. **(C)** Effects of SC optogenetic inhibition on saccade endpoints. Top, scatter plots and

9   histograms of endpoints for control (white background, n = 296) and LED on (orange background, n = 235) trials.

1   Middle, endpoint histograms for control (black) and LED on (orange) trials. Bottom, saccade vectors for control

2   (black) and LED on (orange) trials. **(D)** Head-eye amplitude coupling during ear airpuff-evoked gaze shifts for control

3   (black) and LED on (orange) trials. Each dot represents an individual gaze shift. Control: $R^2 = 0.56$, slope = 0.123, p <

4   10^{-10}. LED on: $R^2 = 0.53$, slope = 0.127, $p < 10^{-10}$. Control and LED on regression slopes were significantly different

5   (p=0.01, permutation test) due to differences in eye positions from which gaze shifts were generated, because

6   controlling for initial eye position eliminated this difference (Supplementary Fig. 10). Histograms above and beside

7   scatter plot show distributions of saccade amplitudes and attempted head displacements, respectively. Distribution

8   means were significantly different ($p < 10^{-5}$, permutation test). **(E)** Schematic of right SC optogenetic subthreshold

9   stimulation using ChR2 and example histology for representative mouse. Scale bar, 0.5 mm. **(F)** Trial structure.

10   Optogenetic illumination is provided for a 1 s period centered around airpuff delivery. **(G)** Effects of weak SC

11   optogenetic stimulation on saccade endpoints. Top, scatter plots and histograms of endpoints for control (white

12   background, n = 547) and LED on (blue background, n = 157) trials. We observed fewer trials in the LED-on condition

13   because SC stimulation increased the probability of spontaneous saccades prior to stimulus onset, and trials with

14   saccades in the 500 ms before stimulus delivery were excluded from analysis. Middle, histograms of endpoints for

15   control (black) and LED on (blue) trials. Bottom saccade vectors for control (black) and LED on (blue) trials. **(H)**

16   Head-eye amplitude coupling during ear airpuff-evoked gaze shifts for control (black) and LED on (blue) trials. Each

17   dot represents an individual gaze shift. Attempted head amplitude was measured 150 ms after saccade onset.

18   Control: $R^2 = 0.69$, slope = 0.137, $p < 10^{-10}$. LED on: $R^2 = 0.52$, slope = 0.164, $p < 10^{-10}$. Control and LED-on

19   regression slopes were significantly different ($p < 10^{-5}$, permutation test) due to difference in eye positions from which

20   gaze shifts were generated, because controlling for initial eye position eliminated this difference (Supplementary Fig.

21   10). Histograms above and beside scatter plot show distributions of saccade amplitudes and attempted head

22   displacements, respectively. Distribution means were significantly different ($p < 10^{-5}$, permutation test).

23

24   To understand how SC manipulations affect attempted head movements and head-eye

25   coupling, we examined the distribution of head movements as a function of saccade amplitude.

26   As expected given the role of SC in generating both head and eye movements, attempted head

27   movements were shifted to the right (*i.e.,* ipsiversively) by SC inhibition (Fig. 4D) and to the left

28   (*i.e.,* contraversively) by SC excitation (Fig. 4H). To examine the effects of SC manipulations on

29   head-eye coupling, we identified trials with identical saccade trajectories in LED-on and LED-off

30   conditions and examined the corresponding head movement amplitudes. Interestingly, SC

1   manipulations had no effect on the relationship between saccade and head movement

2   amplitudes, suggesting that SC manipulations do not change head-eye coupling during gaze

3   shifts. Taken together, these bidirectional manipulations indicate that SC serves a conserved

4   necessary and sufficient role in generating ear airpuff-evoked gaze shifts in which it specifies

5   overall gaze shift amplitude.

6

7   **Discussion:**

8   Here we investigated whether mouse gaze shifts are more diverse than had previously been

9   appreciated. In the prevailing view, mouse gaze shifts are led by head rotations that trigger

10   compensatory eye movements, including saccades that function to reset the eyes (Land, 2019;

11   Land and Nilsson, 2012; Liversedge et al., 2011; Meyer et al., 2020; Michaiel et al., 2020;

12   Payne and Raymond, 2017). These "recentering" saccades are attributed to head movement-

13   related vestibular and optokinetic cues (Curthoys, 2002; Meyer et al., 2020; Michaiel et al.,

14   2020; Payne and Raymond, 2017). Working in a head-fixed context to eliminate vestibular and

15   optokinetic cues and to present stimuli of different modalities at precise craniotopic locations, we

16   found that mice are capable of an additional type of gaze shift. As discussed below, we

17   identified numerous features that distinguish this new type of gaze shift from the previously

18   studied type, including the endpoints of the saccades, their timing and amplitude relative to

19   attempted head movements, and the brain regions that drive them.

20

21   **Touch-evoked saccades are directed**

22   The first indication that touch-evoked gaze shifts differ from those previously observed in mice

23   was an endpoint analysis revealing that touch-evoked saccades are directed rather than

24   recentering. This conclusion is based on three lines of evidence. First, endpoints of saccades

25   evoked by left and right ear airpuffs are near the left and right edges, respectively, of the range

26   of eye positions observed and overlap minimally, despite trial-to-trial variability. In contrast,

1 endpoints for saccades evoked by left and right auditory stimuli are indistinguishable and well

2 described by the recentering model. Second, left and right ear airpuffs evoke saccades traveling

3 in opposite directions from most eye positions; by definition, one of these directions must lead

4 away from center and is thus *centrifugal* rather than *centripetal*. In contrast, saccades evoked by

5 both left and right auditory stimuli travel centripetally from all initial eye positions. Third, from

6 many eye positions, touch-evoked saccades that begin towards the center pass through to

7 reach endpoints at eccentricities between 5 to 10 degrees and cannot accurately be termed

8 centripetal. For these reasons, we conclude that touch-evoked saccades are directed and do

9 not serve to recenter the eyes.

10

11 Our findings contrast with and complement previous studies contending that rodents, like other

12 afoveates, use saccades to reset their eyes to more central locations (Meyer et al., 2018, 2020;

13 Michaiel et al., 2020; Wallace et al., 2013). One recent analysis suggested that gaze shifts

14 made during visually guided prey capture involve resetting centripetal saccades that "catch up"

15 with the head (Michaiel et al., 2020). Another found that saccades away from the nose recenter

16 the eye, whereas saccades toward the nose move the eye slightly beyond center (Meyer et al.,

17 2020). Although we observed this as well, it does not contribute to our results because we

18 averaged the positions of the left and right eyes, eliminating this asymmetry. Earlier studies in

19 head-fixed mice observed occasional, undirected saccades in response to changes in the visual

20 environment (Samonds et al., 2018) and found that mice could be trained to produce visually

21 guided saccades only after weeks of training and at extremely long (~1 s) latencies (Itokazu et

22 al., 2018). To our knowledge, ours is the first study demonstrating innate gaze shifts involving

23 directed saccades in mice (or any species lacking a fovea).

24

25

26

1 **Touch-evoked gaze shifts are not led by head movements**

2 The prevailing view holds that head movements initiate and determine the amplitude of mouse

3 gaze shifts, with eye movements compensatory by-products. In support of this model, one study

4 found that spontaneous saccades in head-fixed mice are preceded by attempted head rotations.

5 A careful comparison with gaze shifts occurring during visually guided object tracking and social

6 interactions in freely moving mice led the authors to suggest that head-eye coupling is not

7 disrupted during head-fixation, and that gaze shifts in both contexts are head-initiated (Meyer et

8 al., 2020). Another study tracked the eyes and head during visually guided cricket hunting and

9 found that gaze shifts are driven by the head, with the eyes following to stabilize and recenter

10 gaze (Michaiel et al., 2020). Together, these findings have bolstered the prevailing view that

11 afoveates such as mice generate gaze shifts driven by head movements, with eye movements

12 compensatory by-products (Land, 2019; Land and Nilsson, 2012; Liversedge et al., 2011).

13 However, while our findings for spontaneous saccades are consistent with those in the

14 literature, we have shown that touch-evoked gaze shifts are initiated by saccades, a finding that

15 contrasts with and complements earlier studies.

16

17 This finding that touch-evoked gaze shifts are initiated by saccades suggests that mouse

18 saccades are not always a simple by-product of head movements. Additional support for this

19 idea came from an analysis of head and eye movements as a function of eye position. If gaze

20 shifts were determined solely by the location of the stimulus relative to the head and saccades

21 were a compensatory by-product of this calculation, eye position should have no effect on head

22 movement amplitude. However, we found that the amplitudes and directions of both saccades

23 and attempted head movements evoked by saccades vary with initial eye position. The

24 influence of eye position on touch-evoked eye *and* head movements further indicates that

25 saccades are not compensatory by-products of head movements. Instead, touch-evoked head

26 movements and directed saccades are specified simultaneously as parts of a coordinated

21

1   movement whose component movements take into account both stimulus location and initial

2   eye position.

3

4   The relative timing of head and eye components during touch-evoked gaze shifts in mice

5   resembles that observed during gaze shifts in cats and primates. For example, head-fixed cats

6   and primates generate gaze shifts using directed saccades and then maintain their eyes in the

7   new orbital position, similar to what we have observed in mice (Freedman, 2008; Guitton et al.,

8   1980). In addition, saccades in head-fixed cats and primates are often accompanied by

9   attempted head rotations, similar to those we observe during touch-evoked gaze shifts in head-

10 fixed mice (Bizzi et al., 1971; Guitton et al., 1984; Paré et al., 1994). In primates and cats able to

11 move their heads, gaze shifts are usually led by directed saccades (with some exceptions),

12 likely because the eyes have lower rotational inertia and can move faster (Pelisson and

13 Guillaume, 2009; Ruhland et al., 2013). These saccades tend to be followed by a head

14 movement in the same direction that creates vestibular signals that drive slow, centripetal

15 counterrotation of the eyes to maintain fixation (Bizzi et al., 1972; Freedman, 2008; Freedman

16 and Sparks, 1997; Guitton et al., 1984). In this way, the animal can rapidly shift its gaze with a

17 directed saccade yet subsequently reset the eyes to a more central position as the head moves.

18 It is tempting to speculate that a similar coordinated sequence of head and eye movements

19 occurs during freely moving touch-evoked gaze shifts, enabling mice to rapidly shift gaze with

20 their eyes while eventually resetting the eyes in a more central orbital position.

21

22 **Head-eye amplitude coupling differs during spontaneous and evoked saccades**

23 An additional feature that distinguishes spontaneous and touch-evoked gaze shifts is the

24 relative contributions of head and eye movements. We found that spontaneous saccades of a

25 given amplitude are coupled to larger head movements than are touch-evoked saccades. This

26 difference arises largely from the absence of a pre-saccadic attempted head movement during

22

1   touch-evoked gaze shifts. This differential pairing of head and eye movements is reminiscent of

2   reports in primates and cats that the relative contributions of head and eye movements vary for

3   gaze shifts evoked by different sensory modalities (Goldring et al., 1996; Populin, 2006; Populin

4   and Rajala, 2011; Populin et al., 2004a; Ruhland et al., 2013; Tollin et al., 2005). However, in

5   those species, vision typically elicits gaze shifts dominated by saccades while hearing typically

6   evokes gaze shifts entailing larger contributions from head movements. In contrast, we

7   observed that sound- and touch-evoked gaze shifts involve larger contributions from saccades

8   than do spontaneous gaze shifts, whereas visual stimuli did not evoke gaze shifts at all. This

9   indicates that although there is general conservation of the involvement of SC in sensory-driven

10 gaze shifts, modality-specific features are not conserved, which may reflect differences in

11 sensory processing across species. For example, virtually every cell in primate intermediate and

12 deep SC that is responsive to tactile stimuli is also responsive to visual stimuli (Groh and

13 Sparks, 1996). In contrast, a recent study of *Pitx2*^{+} neurons in the intermediate and deep mouse

14 SC, which project to brainstem oculomotor centers and when optogenetically stimulated evoke

15 orienting movements of the eyes and head reminiscent of the gaze shifts we describe (Masullo

16 et al., 2019), reported that these neurons responded robustly to whisker airpuffs but did not

17 respond to visual stimuli (Xie et al., 2021). We also observed limited variability across mice in

18 the relative contributions of head and eye movements to gaze shifts, which contrasts with the

19 observation that different human subjects are head "movers" and "non-movers" during gaze

20 shifts (Supplementary Fig. 9) Thus, our results reveal that mice are capable of using multiple

21 strategies to shift their gaze but with key differences from other species.

22

23 **The role of superior colliculus in sensory-evoked mouse gaze shifts**

24 In other species, SC drives sensory-evoked gaze shifts, and microstimulation and optogenetic

25 stimulation of mouse SC has been shown to elicit gaze shifts (Masullo et al., 2019; Wang et al.,

26 2015). However, to our knowledge, no study had identified a causal involvement of SC in mouse

23

1   gaze shifts. We performed bidirectional optogenetic manipulations that revealed that touch-

2   evoked gaze shifts depend on SC, identifying a conserved, necessary and sufficient role for SC

3   in directed gaze shifts. In addition, we found that SC manipulations did not alter head-eye

4   amplitude coupling. This observation suggests that SC specifies the overall gaze shift amplitude

5   rather than the individual eye or head movement components, consistent with observations in

6   other species (Freedman et al., 1996; Paré et al., 1994).

7

8   **Ethological significance**

9   Prior to the present study, it was believed that species with high-acuity retinal specializations

10   acquired the ability to make directed saccades to scrutinize salient environmental stimuli,

11   because animals lacking such retinal specializations were thought incapable of gaze shifts led

12   by directed saccades (Land, 2019; Land and Nilsson, 2012; Liversedge et al., 2011; Walls,

13   1962). Our discovery that sensory-guided directed saccades are present in mice—albeit without

14   the precise targeting of stimulus location seen in foveate species—raises the question of what

15   fovea-independent functions these movements serve. Although mice have lateral eyes and a

16   large field of view, saccades that direct gaze towards a stimulus, as seems to occur with both

17   ear and whisker tactile stimuli, may facilitate keeping salient stimuli within the field of view. As

18   natural stimuli are often multimodal, directing non-visual stimuli towards the center of view

19   maximizes the likelihood of detecting the visual component of the stimulus. Alternatively, despite

20   mouse retinae lacking discrete, anatomically defined specializations such as foveae or areas

21   centralis, there are subtler nonuniformities in the distribution and density of photoreceptors and

22   retinal ganglion cell subtypes, and magnification factor, receptive field sizes, and response

23   tuning vary across the visual field in higher visual centers; it may be desirable to center a salient

24   tactile stimulus on a particular retinal region to enable scrutiny of the visual component of the

25   stimulus (Ahmadlou and Heimel, 2015; Baden et al., 2013; van Beest et al., 2021; Bleckert et

26   al., 2014; Drager and Hubel, 1976; Feinberg and Meister, 2015; Li et al., 2020; de Malmazet et

24

1 al., 2018). Although touch-evoked saccades alone may be too small to center the stimulus

2 location on any particular region of the retina, they may do so in concert with directed head

3 movements.

4

5 Why tactile stimuli evoked directed saccades in our preparation whereas auditory and visual

6 stimuli do not is unclear. One possibility is the aforementioned speed of saccades relative to

7 head movements may be especially beneficial because tactile stimuli typically derive from

8 proximal objects and as a result may demand rapid responses. Alternatively, because the

9 spatial acuity of the tactile system is higher than that of the auditory system in mice, this may

10 enable more precise localization of the tactile stimuli (Allen and Ison, 2010; Diamond et al.,

11 2008). Auditory stimuli, in contrast, may alert animals to the presence of a salient stimulus in

12 their environments whose location is less precisely ascertained, and as a result drive gaze shifts

13 whose goal is to reset the eyes to a central position that maximizes their chances of sensing

14 and responding appropriately. Finally, our set of stimuli was not exhaustive, and it is possible

15 that as yet unidentified visual or auditory stimuli could elicit gaze shifts with directed saccades.

16 Alternatively, the recent report that mouse SC *Pitx2*^{+} neurons respond to tactile but not visual

17 stimuli may indicate that visual orienting is driven by a distinct neural pathway or that head-fixing

18 gates visual but not tactile responses of SC neurons.

19

20 **Future Directions**

21 In this study we used a head-fixed preparation to eliminate the confound of head movement-

22 related sensory cues and to present stimuli from defined locations. However, in the future, it will

23 be interesting to compare touch-evoked gaze shifts in head-fixed and freely moving animals.

24 For example, as noted previously, whereas head-fixed primates and cats generate gaze shifts

25 using directed saccades and then maintain their eyes in the new orbital position, similar to what

26 we have observed, in freely moving primates and cats, gaze shifts are led by directed saccades

25

1 but typically followed by head movements during which the eyes counterrotate centripetally in

2 order to maintain gaze in the new direction. It will be interesting to know whether similar

3 differences distinguish saccade-led touch-evoked gaze shifts in head-fixed and freely moving

4 mice. By expanding on methods recently described by other groups, it may be possible to

5 investigate these and other questions (Meyer et al., 2018, 2020; Michaiel et al., 2020; Payne

6 and Raymond, 2017).

7

8 Furthermore, a practical implication of our identification of mouse SC-dependent gaze shifts is

9 that this behavioral paradigm could be applied to the study of several outstanding questions.

10 First, there are many unresolved problems regarding the circuitry and ensemble dynamics

11 underlying target selection (Basso and May, 2017) and saccade generation (Gandhi and

12 Katnani, 2011), and the mouse provides a genetically tractable platform with which to

13 investigate these and other topics. Second, gaze shifts are aberrant in a host of conditions, such

14 as Parkinson's and autism spectrum disorder (Liversedge et al., 2011). This paradigm could be

15 a powerful tool for the study of mouse models of a variety of neuropsychiatric conditions. Third,

16 directing saccades towards particular orbital positions during these gaze shifts requires an

17 ability to account for the initial positions of the eyes relative to the target, a phenomenon also

18 known as remapping from sensory to motor reference frames. Neural correlates of this process

19 have been observed in primates (Groh and Sparks, 1996; Jay and Sparks, 1984) and cats

20 (Populin et al., 2004b), but the underlying circuitry and computations remain obscure. This

21 behavior may facilitate future studies of this problem. Fourth, the different types of gaze shifts

22 that rely on distinct head-eye coupling we have identified may be useful for understanding

23 mechanisms that control movement coordination. Thus, touch-evoked saccade behavior is likely

24 to be a powerful tool for myriad lines of investigation.

25

26

26

1   **Conclusions**

2   We have found that mice make an unexpectedly broad range of gaze shifts, including a new

3   type that is elicited by sensory stimuli, led by directed saccades, and incorporates smaller head

4   movements. Prior studies in species whose retinae lack high-acuity specializations had never

5   observed this type of gaze shift, but our study used a broader range of stimuli than previously

6   tested in a preparation that allowed spatially precise delivery. Detailed perturbation experiments

7   determined that the circuit mechanisms of sensory-evoked gaze shifts are conserved from mice

8   to primates, suggesting that this behavior may have arisen in a common, afoveate ancestral

9   species long ago. More broadly, our findings suggest that analyzing eye movements of other

10   afoveate species thought not to make directed saccades—such as rabbits, toads, and

11   goldfish—in response to a diverse range of multimodal stimuli may uncover similar abilities to

12   make diverse types of gaze shifts.

13

21

22   **Author contributions:** S.H.Z., D.E.T., and E.H.F. conceived of the project, designed the

23   experiments, analyzed the data, and prepared the manuscript. S.H.Z., D.E.T., J.Y.W., and

24   J.M.A. conducted the experiments.

25

26   **Competing interests:** The authors declare no competing interests.

References:

Ahmadlou, M., and Heimel, J.A. (2015). Preference for concentric orientations in the mouse superior colliculus. Nat. Commun. *6*, 1–11.

Allen, P.D., and Ison, J.R. (2010). Sensitivity of the mouse to changes in azimuthal sound location: Angular separation, spectral composition, and sound level. Behav. Neurosci. *124*, 265.

Baden, T., Schubert, T., Chang, L., Wei, T., Zaichuk, M., Wissinger, B., and Euler, T. (2013). A tale of two retinal domains: Near-Optimal sampling of achromatic contrasts in natural scenes through asymmetric photoreceptor distribution. Neuron *80*, 1206–1217.

Bahill, A.T., Clark, M.R., and Stark, L. (1975). The main sequence, a tool for studying human eye movements. Math. Biosci. *24*, 191–204.

Basso, M.A., and May, P.J. (2017). Circuits for Action and Cognition: A View from the Superior Colliculus.

van Beest, E.H., Mukherjee, S., Kirchberger, L., Schnabel, U.H., van der Togt, C., Teeuwen, R.R.M., Barsegyan, A., Meyer, A.F., Poort, J., Roelfsema, P.R., et al. (2021). Mouse visual cortex contains a region of enhanced spatial resolution. Nat. Commun. 2021 121 *12*, 1–17.

Bizzi, E., Kalil, R., and Tagliasco, V. (1971). Eye-head coordination in monkeys: evidence for centrally patterned organization. Science *173*, 452–454.

Bizzi, E., Kalil, R.E., and Morasso, P. (1972). Two modes of active eye-head coordination in monkeys. Brain Res. *40*, 45–48.

Bleckert, A., Schwartz, G.W., Turner, M.H., Rieke, F., and Wong, R.O.L. (2014). Visual space is represented by nonmatching topographies of distinct mouse retinal ganglion cell types. Curr. Biol. *24*, 310–315.

Curthoys, I.S. (2002). Generation of the quick phase of horizontal vestibular nystagmus. Exp. Brain Res. 2002 1434 *143*, 397–405.

Diamond, M.E., von Heimendahl, M., Knutsen, P.M., Kleinfeld, D., and Ahissar, E. (2008).

"Where" and "what" in the whisker sensorimotor system. Nat. Rev. Neurosci. 2008 98 *9*, 601–612.

Drager, U.C., and Hubel, D.H. (1975). Responses to visual stimulation and relationship between visual, auditory, and somatosensory inputs in mouse superior colliculus. J. Neurophysiol. *38*, 690–713.

Drager, U.C., and Hubel, D.H. (1976). Topography of visual and somatosensory projections to mouse superior colliculus. J. Neurophysiol. *39*, 91-101.

Feinberg, E.H., and Meister, M. (2015). Orientation columns in the mouse superior colliculus. Nature *519*, 229–232.

Freedman, E.G. (2008). Coordination of the Eyes and Head during Visual Orienting. Exp. Brain Res. *190*, 369.

Freedman, E., and Sparks, D. (1997). Eye-head coordination during head-unrestrained gaze shifts in rhesus monkeys. J. Neurophysiol. *77*, 2328–2348.

Freedman, E., Stanford, T., and Sparks, D. (1996). Combined eye-head gaze shifts produced by electrical stimulation of the superior colliculus in rhesus monkeys. J. Neurophysiol. *76*, 927–952.

Gandhi, N.J., and Katnani, H.A. (2011). Motor Functions of the Superior Colliculus. Annu. Rev. Neurosci. *34*, 205–231.

Goldring, J.E., Dorris, M.C., Corneil, B.D., Ballantyne, P., and Munoz, D. (1996). Combined eye-head gaze shifts to visual and auditory targets in humans (Springer-Verlag).

Gradinaru, V., Zhang, F., Ramakrishnan, C., Mattis, J., Prakash, R., Diester, I., Goshen, I., Thompson, K.R., and Deisseroth, K. (2010). Molecular and Cellular Approaches for Diversifying and Extending Optogenetics. Cell *141*, 154–165.

Groh, J.M., and Sparks, D.L. (1996). Saccades to somatosensory targets. III. eye-position-dependent somatosensory activity in primate superior colliculus. J. Neurophysiol. *75*, 439–453.

Guitton, D. (1992). Control of eye-head coordination during orienting gaze shifts. Trends

Neurosci. *15*, 174–179.

Guitton, D., Crommelinck, M., and Roucoux, A. (1980). Stimulation of the superior colliculus in the alert cat. I. Eye movements and neck EMG activity evoked when the head is restrained. Exp. Brain Res. *39*, 63–73.

Guitton, D., Douglas, R.M., and Volle, M. (1984). Eye-Head Coordination in Cats. J. Neurophysiol. *52*.

Hepp, K., Opstal, A.J. Van, Straumann, D., Hess, B.J., and Henn, V. (1993). Monkey superior colliculus represents rapid eye movements in a two-dimensional motor map. Https://Doi.Org/10.1152/Jn.1993.69.3.965 *69*, 965–979.

Hikosaka, O., and Wurtz, R.H. (1985). Modification of saccadic eye movements by GABA-related substances. I. Effect of muscimol and bicuculline in monkey superior colliculus. J. Neurophysiol. *53*, 266–291.

Itokazu, T., Hasegawa, M., Kimura, R., Osaki, H., Albrecht, U.R., Sohya, K., Chakrabarti, S., Itoh, H., Ito, T., Sato, T.K., et al. (2018). Streamlined sensory motor communication through cortical reciprocal connectivity in a visually guided eye movement task. Nat. Commun. *9*, 1–14.

Jay, M.F., and Sparks, D.L. (1984). Auditory receptive fields in primate superior colliculus shift with changes in eye position. Nature *309*, 345–347.

Kitama, T., Ohki, Y., Shimazu, H., Tanaka, M., and Yoshida, K. (1995). Site of interaction between saccade signals and vestibular signals induced by head rotation in the alert cat: functional properties and afferent organization of burster-driving neurons. J. Neurophysiol. *74*, 273–287.

Land, M.F. (2019). The Evolution of Gaze Shifting Eye Movements. In Current Topics in Behavioral Neurosciences, (Springer), pp. 3–11.

Land, M.F., and Nilsson, D.-E. (2012). Animal Eyes (Oxford Univerity Press).

Lee, C. (1999). Eye and head coordination in reading: roles of head movement and cognitive control. Vision Res. *39*, 3761–3768.

1 Li, Y. tang, Turan, Z., and Meister, M. (2020). Functional Architecture of Motion Direction in the

2 Mouse Superior Colliculus. Curr. Biol. *30*, 3304–3315.

3 Liversedge, S.P., Gilchrist, I.D., and Everling, S. (2011). The Oxford Handbook of Eye

4 Movements (Oxford Univerity Press).

5 de Malmazet, D., Kühn, N.K., and Farrow, K. (2018). Retinotopic Separation of Nasal and

6 Temporal Motion Selectivity in the Mouse Superior Colliculus. Curr. Biol. *28*, 2961-2969.e4.

7 Masullo, L., Mariotti, L., Alexandre, N., Freire-Pritchett, P., Boulanger, J., and Tripodi, M. (2019).

8 Genetically Defined Functional Modules for Spatial Orienting in the Mouse Superior Colliculus.

9 Curr. Biol. *29*.

10 May, P.J. (2006). The mammalian superior colliculus: laminar structure and connections. Prog.

11 Brain Res. *151*.

12 Meyer, A.F., Poort, J., O'Keefe, J., Sahani, M., and Linden, J.F. (2018). A Head-Mounted

13 Camera System Integrates Detailed Behavioral Monitoring with Multichannel Electrophysiology

14 in Freely Moving Mice. Neuron *100*, 46-60.e7.

15 Meyer, A.F., O'Keefe, J., and Poort, J. (2020). Two Distinct Types of Eye-Head Coupling in

16 Freely Moving Mice. Curr. Biol. *30*, 2116-2130.e6.

17 Michaiel, A.M., Abe, E.T.T., and Niell, C.M. (2020). Dynamics of gaze control during prey

18 capture in freely moving mice. Elife *9*, 1–27.

19 Paré, M., and Munoz, D.P. (2001). Expression of a re-centering bias in saccade regulation by

20 superior colliculus neurons. Exp. Brain Res.

21 Paré, M., Crommelinck, M., and Guitton, D. (1994). Gaze shifts evoked by stimulation of the

22 superior colliculus in the head-free cat conform to the motor map but also depend on stimulus

23 strength and fixation activity. Exp. Brain Res. *101*, 123–139.

24 Payne, H.L., and Raymond, J.L. (2017). Magnetic eye tracking in mice. Elife *6*.

25 Pelisson, D., and Guillaume, A. (2009). Eye-Head Coordination. Encycl. Neurosci. 1545–1548.

26 Populin, L.C. (2006). Monkey Sound Localization: Head-Restrained versus Head-Unrestrained

1   Orienting. J. Neurosci. *26*, 9820–9832.

2   Populin, L.C., and Rajala, A.Z. (2011). Target modality determines eye-head coordination in

3   nonhuman primates: Implications for gaze control. J. Neurophysiol. *106*, 2000–2011.

4   Populin, L.C., Tollin, D.J., and Yin, T.C.T. (2004a). Effect of Eye Position on Saccades and

5   Neuronal Responses to Acoustic Stimuli in the Superior Colliculus of the Behaving Cat. J.

6   Neurophysiol. *92*, 2151–2167.

7   Populin, L.C., Tollin, D.J., and Yin, T.C.T. (2004b). Effect of eye position on saccades and

8   neuronal responses to acoustic stimuli in the superior colliculus of the behaving cat. J.

9   Neurophysiol. *92*, 2151–2167.

10   Reimer, J., Froudarakis, E., Cadwell, C.R., Yatsenko, D., Denfield, G.H., and Tolias, A.S.

11   (2014). Pupil Fluctuations Track Fast Switching of Cortical States during Quiet Wakefulness.

12   Neuron *84*, 355–362.

13   Robinson, D.A. (1972). Eye movements evoked by collicular stimulation in the alert monkey.

14   Vision Res. *12*, 1795–1808.

15   Ruhland, J.L., Yin, T.C.T., and Tollin, D.J. (2013). Gaze shifts to auditory and visual stimuli in

16   cats. JARO - J. Assoc. Res. Otolaryngol. *14*, 731–755.

17   Samonds, J.M., Geisler, W.S., and Priebe, N.J. (2018). Natural image and receptive field

18   statistics predict saccade sizes. Nat. Neurosci. *21*, 1591–1599.

19   Schiller, P.H., and Stryker, M. (1972). Single-unit recording and stimulation in superior colliculus

20   of the alert rhesus monkey. J. Neurophysiol. *35*, 915–924.

21   Sparks, D.L. (1986). Translation of sensory signals into commands for control of saccadic eye

22   movements: role of primate superior colliculus. Physiol Rev. *66*, 118–171.

23   Sparks, D.L. (2002). The brainstem control of saccadic eye movements. Nat. Rev. Neurosci. *3*,

24   952–964.

25   Tatler, B.W. (2007). The central fixation bias in scene viewing: Selecting an optimal viewing

26   position independently of motor biases and image feature distributions. J. Vis. *7*, 4.

Tollin, D.J., Populin, L.C., Moore, J., Ruhland, J.L., and Yin, T.C.T. (2005). Sound-localization performance in the cat: the effect of restraining the head. J. Neurophysiol. *93*, 1223–1234.

Wallace, D.J., Greenberg, D.S., Sawinski, J., Rulla, S., Notaro, G., and Kerr, J.N.D. (2013). Rats maintain an overhead binocular field at the expense of constant fusion. Nature *498*, 65–69.

Walls, G.L. (1962). The evolutionary history of eye movements. Vision Res. *2*, 69–80.

Wang, L., Liu, M., Segraves, M.A., and Cang, J. (2015). Visual experience is required for the development of eye movement maps in the mouse superior colliculus. J. Neurosci. *35*, 12281–12286.

Xie, Z., Wang, M., Liu, Z., Shang, C., Zhang, C., Sun, L., Gu, H., Ran, G., Pei, Q., Ma, Q., et al. (2021). Transcriptomic encoding of sensorimotor transformation in the midbrain. Elife *10*.

Zangemeister, W.H., and Stark, L. (1982). Types of gaze movement: Variable interactions of eye and head movements. Exp. Neurol. *77*, 563–577.

1
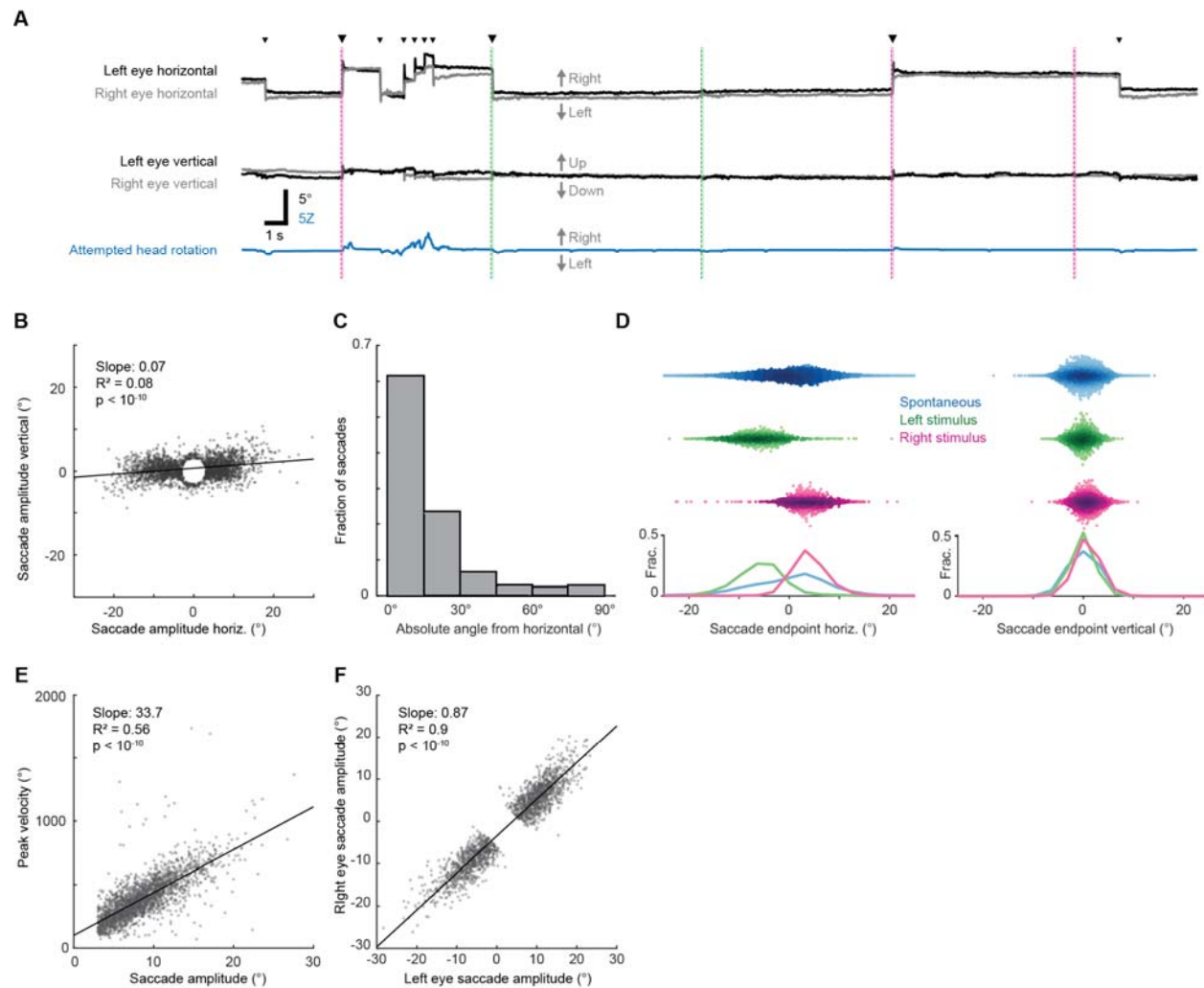
2   **Supplementary Figure 1. Airpuffs evoke horizontal saccades. (A)** Sample traces showing pupil azimuth (top) and

3   elevation (middle) and attempted head rotation (bottom). Black corresponds to left eye, gray corresponds to right eye.

4   Small arrowheads indicate spontaneous saccades. Large arrowheads indicate stimulus-evoked directed saccades.

5   Green and magenta dashed vertical lines correspond to left and right ear airpuffs, respectively. **(B)** Ear airpuff-evoked

6   saccade endpoints and linear fit. n = 5 mice, 2337 trials. **(C)** Distribution of angles between airpuff-evoked saccade

7   vectors and horizontal axis. Gray bars indicate population means. n = 5 mice, 2337 trials **(D)** Distributions of saccade

8   endpoints in horizontal and vertical axes. n = 5 mice; trials = 16291 (spontaneous), 1067 (left airpuff), 1270 (right

9   airpuff**). (E)** Relationship between saccade amplitude and peak velocity**. (F)** Relationship between right and left eye

10   saccade amplitudes. n = 4 mice, 1861 trials.

11

12

1
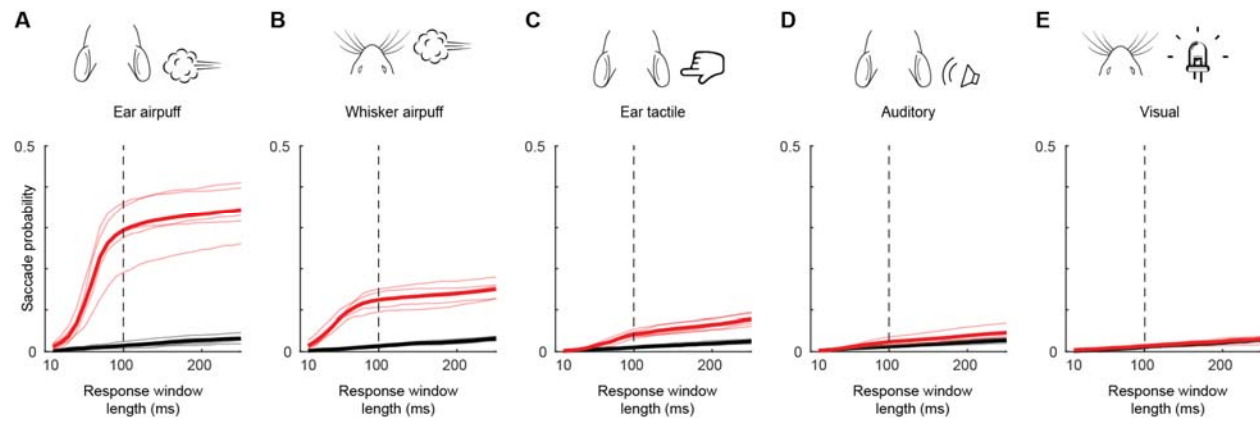
Supplementary Figure 2. Evoked saccades occur within a narrow window after stimulus delivery. (A-E)

Cumulative probabilities of detecting evoked (red) and spontaneous (black) saccades as a function of response

window length for ear airpuffs (A), whisker airpuffs (B), ear tactile stimuli (C), auditory airpuffs (D), and visual stimuli

(E). Thin lines denote values for individual mice, thick lines denote population mean. Dashed vertical line indicates

end of window used for analyses of evoked saccades.

A
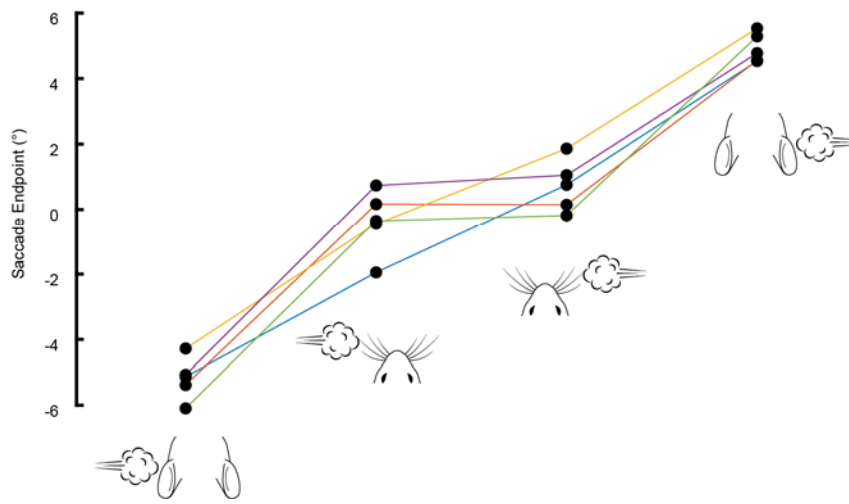
Supplementary Figure 3. Endpoints of airpuff-evoked saccades are ordered according to site of stimulation.

Each line corresponds to a single mouse and shows mean endpoint of saccades evoked by (in order, from left to right) left ear airpuffs, left whisker airpuffs, right whisker airpuffs, and right ear airpuffs).

1
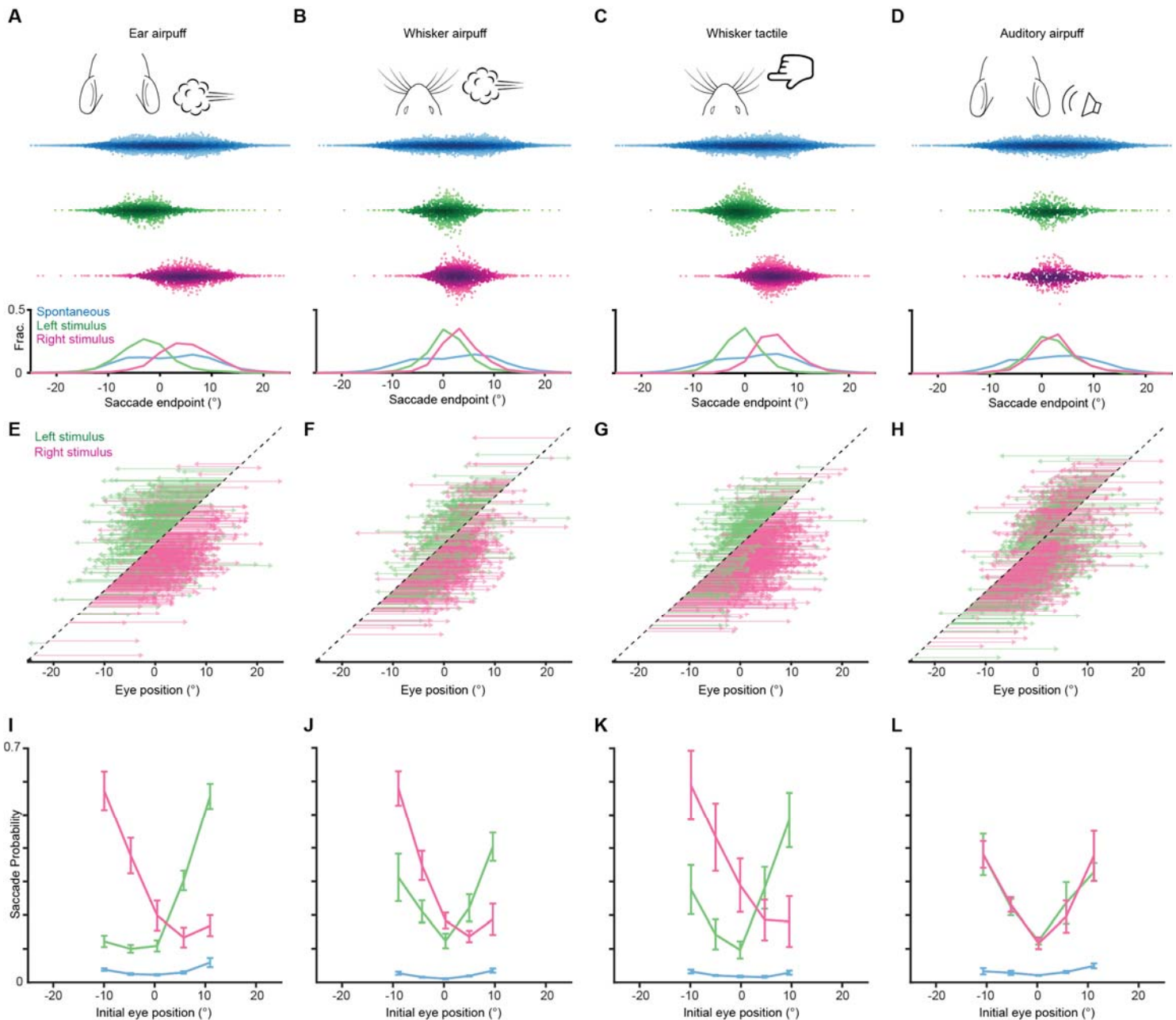
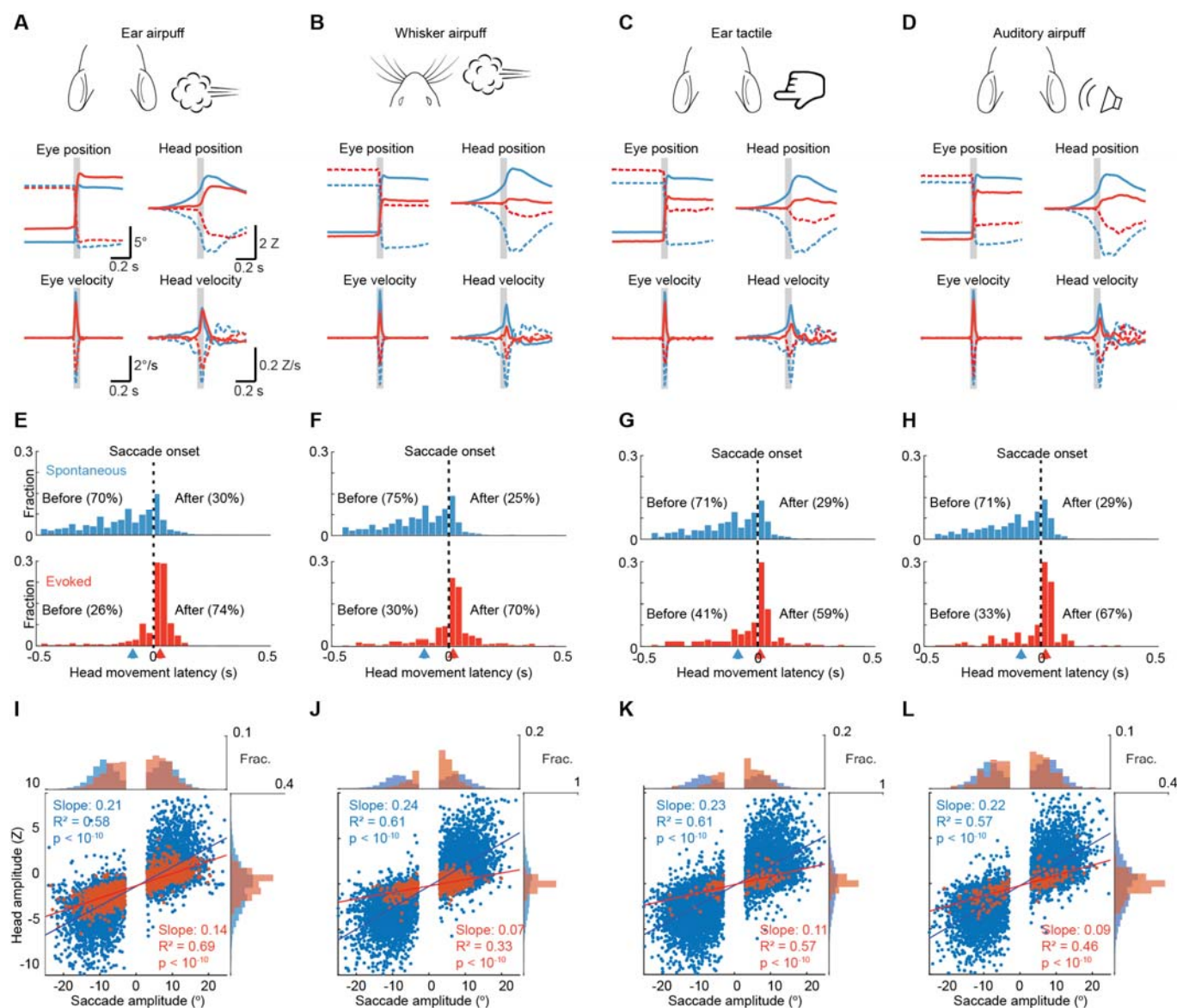**Supplementary Figure 4. Endpoints and trajectories of sensory-evoked saccades for an additional cohort of mice. (A-D)** Endpoints for ear airpuff-, whisker airpuff-, ear tactile-, and auditory airpuff-evoked saccades. Top, schematics of stimuli. Middle, scatter plots showing endpoints of all saccades for all animals made spontaneously (blue) and in response to left (green) and right (magenta) stimuli. Darker shading indicates areas of higher density. Bottom, endpoint distributions for spontaneous and evoked saccades. **(E-H)** Trajectories of individual stimulus-evoked saccades. Each arrow denotes the trajectory of a single saccade. Saccades are sorted according to initial eye positions, which fall on the dashed diagonal line. Saccade endpoints are indicated by arrowheads. Because the

1   probability of evoked gaze shifts differed across stimuli, data are randomly subsampled to show roughly equal

2   numbers of trials for each condition. **(I-L)** Relationship between eye position and saccade probability. Green and

3   magenta lines indicate population means for saccades evoked by left and right stimuli, respectively. Blue lines

4   indicate spontaneous saccades. Error bars indicate s.e.m Saccade numbers for A-L: ear airpuff sessions,

5   spontaneous = 14304, left ear airpuff-evoked = 1221 (244 in E), right ear airpuff-evoked = 1755 (351 in E); whisker

6   airpuff sessions, spontaneous = 8971, left whisker airpuff-evoked = 1107 (221 in F), right whisker airpuff-evoked =

7   1482 (296 in F); whisker tactile sessions, spontaneous = 13242, left whisker-evoked = 1473 (294 in G), right whisker-

8   evoked = 2408 (481 in G); auditory sessions, spontaneous = 8774, left auditory-evoked = 833 (333 in H), right

9   auditory-evoked = 757 (302 in H).

10

11
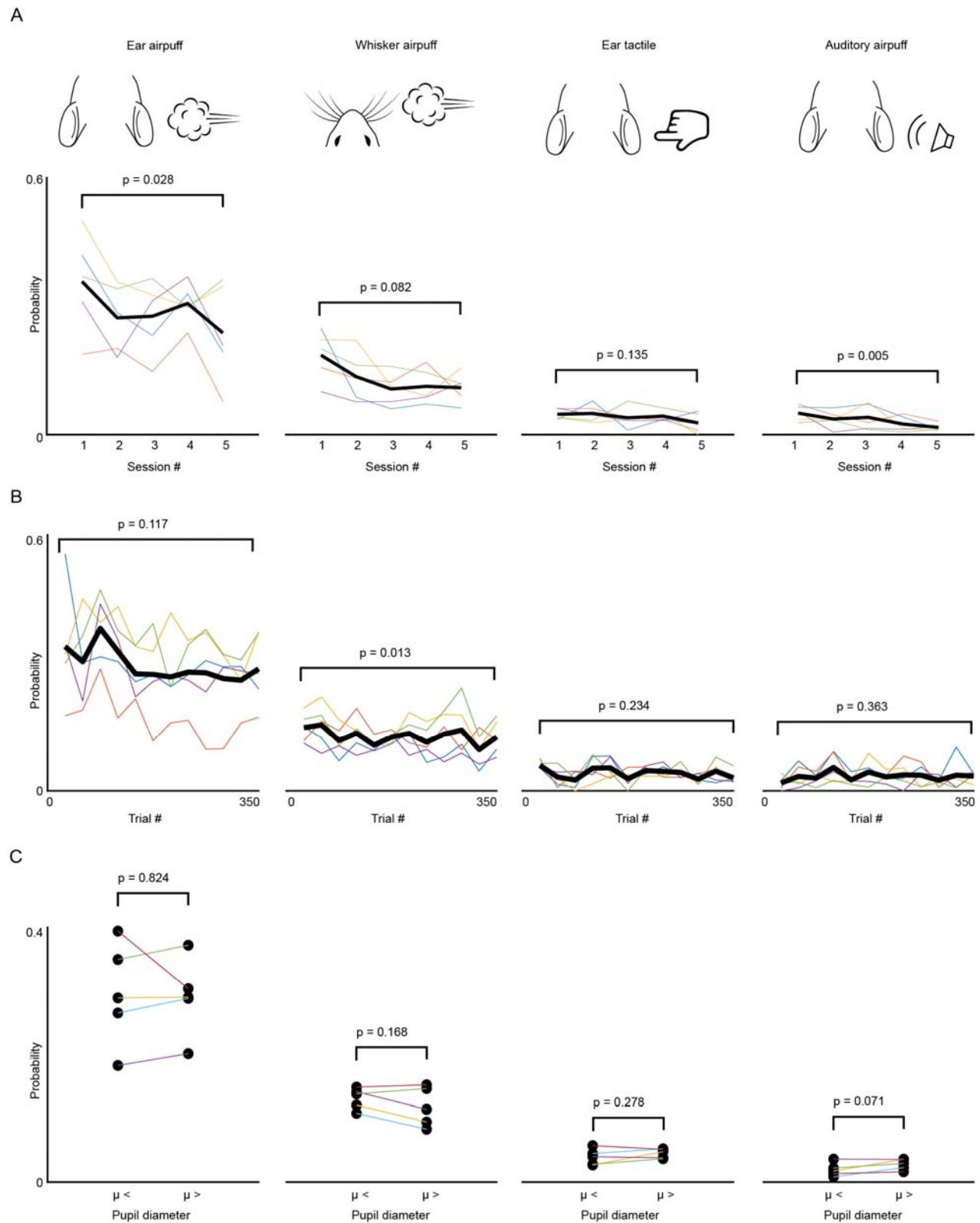
Supplementary Figure 5. Effects of sensory history and arousal on saccade generation. (**A**) Overall gaze shift probability across 5 sessions for ear airpuffs, whisker airpuffs, ear tactile, and auditory airpuffs stimuli. Each thin

39

1   colored line corresponds to an individual mouse. Black line corresponds to mean (**B**) As in (A) but for gaze shift

2   probability within sessions. **(C)** Effects of arousal on saccade probability. μ denotes mean pupil diameter. Statistical

3   significance assessed using paired Student's t-test.

4

Supplementary Figure 6. Head-eye coupling for different stimuli. (A) Top, stimulus schematics. Middle left, mean

trajectories of rightward (solid traces) and leftward (dashed traces) saccades during spontaneous (blue, n= 7146) and

ear airpuff-evoked (red, n = 1437) gaze shifts. Middle right, mean attempted head displacement accompanying

rightward (solid traces) and leftward (dashed traces) saccades during spontaneous (blue) and ear airpuff-evoked

(red) gaze shifts. Bottom left, mean velocities of all rightward (solid traces) and leftward (dashed traces) saccades

during spontaneous (blue) and ear airpuff-evoked (red) gaze shifts. Bottom right, mean attempted head movement

velocities accompanying rightward (solid traces) and leftward (dashed traces) saccades during spontaneous (blue)

and ear airpuff-evoked (red) gaze shifts. **(B-D)** As in (A) for whisker airpuffs (B), ear tactile (C) and auditory airpuffs

(D). n = 5 mice. Trial numbers: whisker airpuff sessions (spontaneous = 7790, evoked = 628), ear tactile sessions

1   (spontaneous = 6706, evoked = 187), auditory airpuff sessions (spontaneous = 10240, evoked = 148). (**E-H**)

2   Distributions of attempted head movement latencies relative to saccade onset for spontaneous (top) and evoked

3   (bottom) saccades. Medians indicated by blue and red arrowheads (ear airpuff sessions, spontaneous: -90 ms,

4   evoked: 30 ms; whisker airpuff sessions, spontaneous: -110 ms, evoked: 20 ms; ear tactile sessions, spontaneous: -

5   90 ms, evoked: 20 ms; auditory sessions, spontaneous: -90ms, evoked: 10 ms) For each condition, distributions are

6   significantly different for spontaneous and evoked gaze shifts ($p < 10^{-5}$, permutation test) (**I-L**). Head-eye amplitude

7   coupling of spontaneous (blue) and evoked saccades (red). Each dot corresponds to a single gaze shift. Regression

8   statistics in figure. For every stimulus type, spontaneous and evoked regression slopes were significantly different (p

9    $< 10^{-5}$, permutation test). Histograms above and beside scatter plot indicate distributions of saccade and attempted

10   head movement amplitudes, respectively. For each condition, distributions were significantly different between

11   spontaneous and evoked ($p < 10^{-5}$, permutation test).

12

1
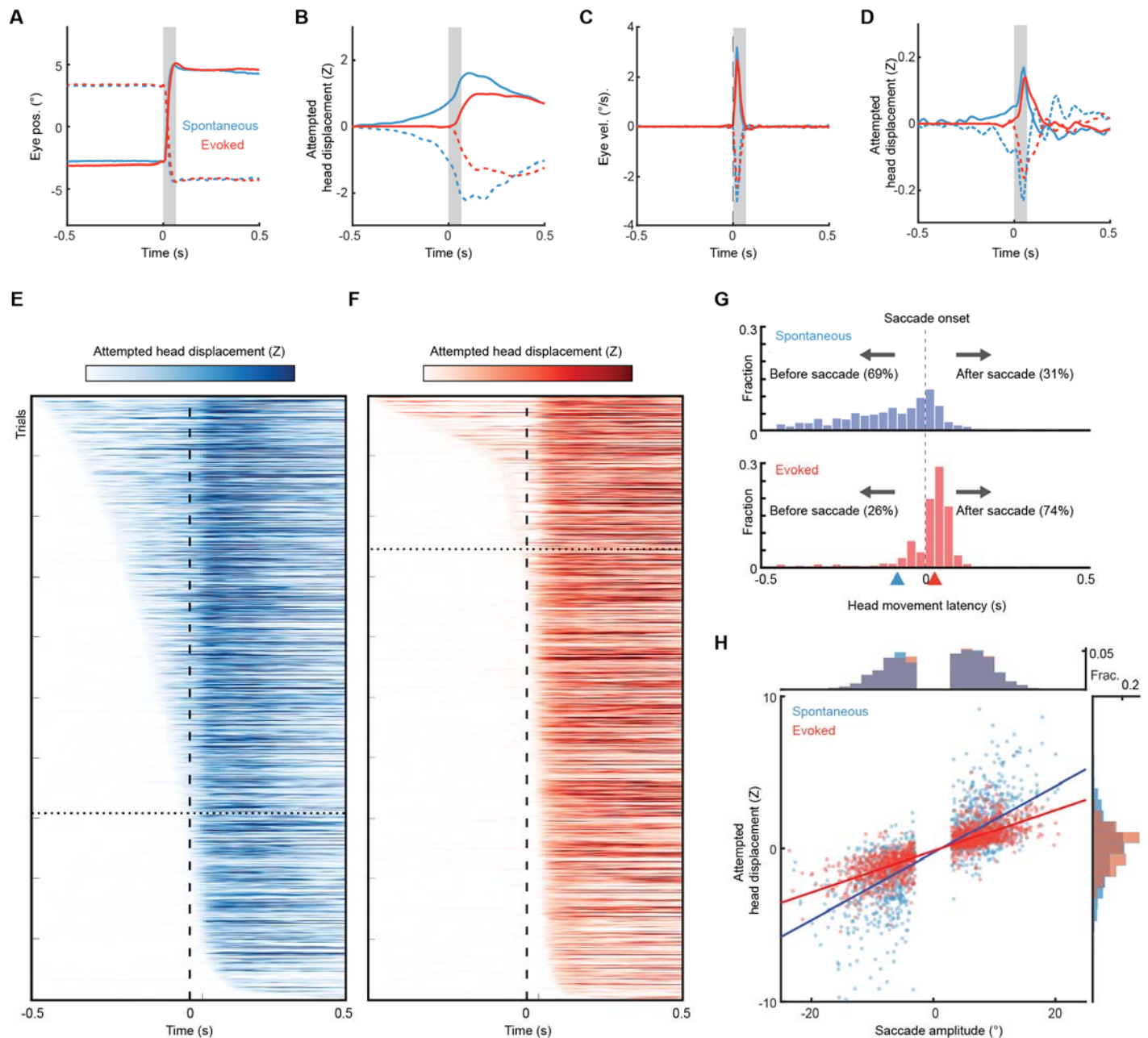
Supplementary Figure 7. Different head-eye coupling during spontaneous and touch-evoked gaze shifts is not due to differences in gaze shift amplitudes. (A) Mean trajectories of amplitude and initial position-matched rightward (solid traces) and leftward (dashed traces) saccades during spontaneous (blue, n= 1437) and ear airpuff-evoked (red, n = 1437) gaze shifts. **(B)** Mean attempted head movement amplitudes accompanying rightward (solid traces) and leftward (dashed traces) saccades during spontaneous (blue) and ear airpuff-evoked (red) gaze shifts. **(C)** Mean velocities of all rightward (solid traces) and leftward (dashed traces) saccades during spontaneous (blue) and ear airpuff-evoked (red) gaze shifts. (**D**) Mean head movement velocities accompanying rightward (solid traces)

43

1   and leftward (dashed traces) saccades during spontaneous (blue) and ear airpuff-evoked (red) gaze shifts. **(E, F)**

2   Timing of attempted head movements relative to saccades during all spontaneous (E) and ear airpuff-evoked (F)

3   gaze shifts. Each row corresponds to a single gaze shift. Darker shades indicate larger attempted head displacement.

4   Dashed vertical line indicates time of saccade onset. Trials are sorted by latency of attempted head movements.

5   Trials above and below dashed horizontal line correspond to attempted head movements that began before and after

6   the saccade, respectively. **(G)** Distributions of attempted head movement latencies relative to saccade onset for

7   spontaneous (top) and ear airpuff-evoked (bottom) saccades. Arrowheads indicate median latencies. **(H)**. Head-eye

8   amplitude coupling of spontaneous (blue) and ear airpuff-evoked saccades (red). Each dot corresponds to a single

9   gaze shift. Attempted head amplitude was measured 150 ms after saccade onset. Spontaneous: $R^2 = 0.60$, slope =

10   0.224, $p < 10^{-10}$. Evoked: $R^2 = 0.69$, slope = 0.135, $p < 10^{-10}$. Spontaneous and evoked regression slopes were

11   significantly different ($p < 10^{-5}$, permutation test). Histograms above and beside scatter plot indicate distributions of

12   saccade and attempted head movement amplitudes. Difference in means were not significant ($p = 0.46$ for saccades,

13 $p = 0.31$ for head, permutation test).

14

1
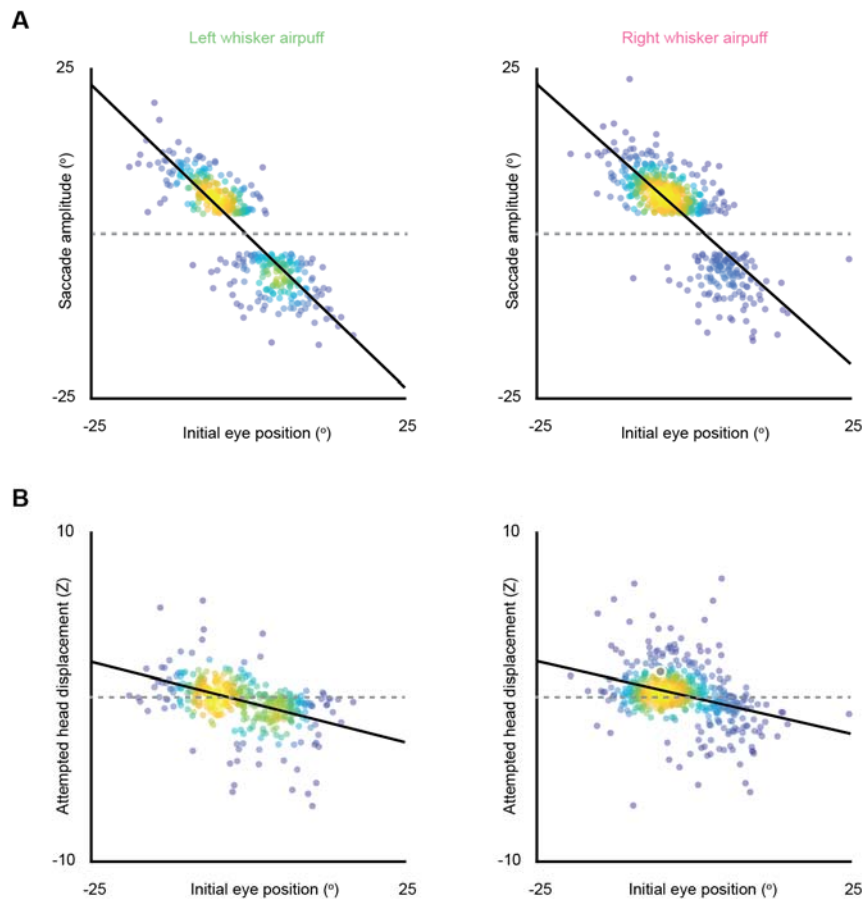
Supplementary Figure 8. Whisker-evoked saccade and attempted head movement direction and amplitude

vary according to initial eye position. (A) Saccade amplitude as a function of initial eye position for left and right

whisker airpuff-evoked gaze shift. Each dot corresponds to a single saccade. Brighter areas indicate higher densities

of points. Linear fits for left and right airpuffs, respectively: slope = -0.92 and -0.85, R^2 = 0.74 and 0.63, $p < 10^{-10}$ and

$p < 10^{-10}$, n = 441 and 606. **(B)** Attempted head movement amplitude as a function of initial eye position for left and

right whisker airpuff-evoked gaze shifts. Linear fits for left and right airpuffs, respectively: slope = -0.10 and -0.09, R^2

= 0.19 and 0.13, $p < 10^{-10}$ and $p < 10^{-10}$, n = 441 and 606. Dashed lines correspond to 0. Values above and below

dashed line correspond to attempted rightward and leftward movements, respectively.

10

1
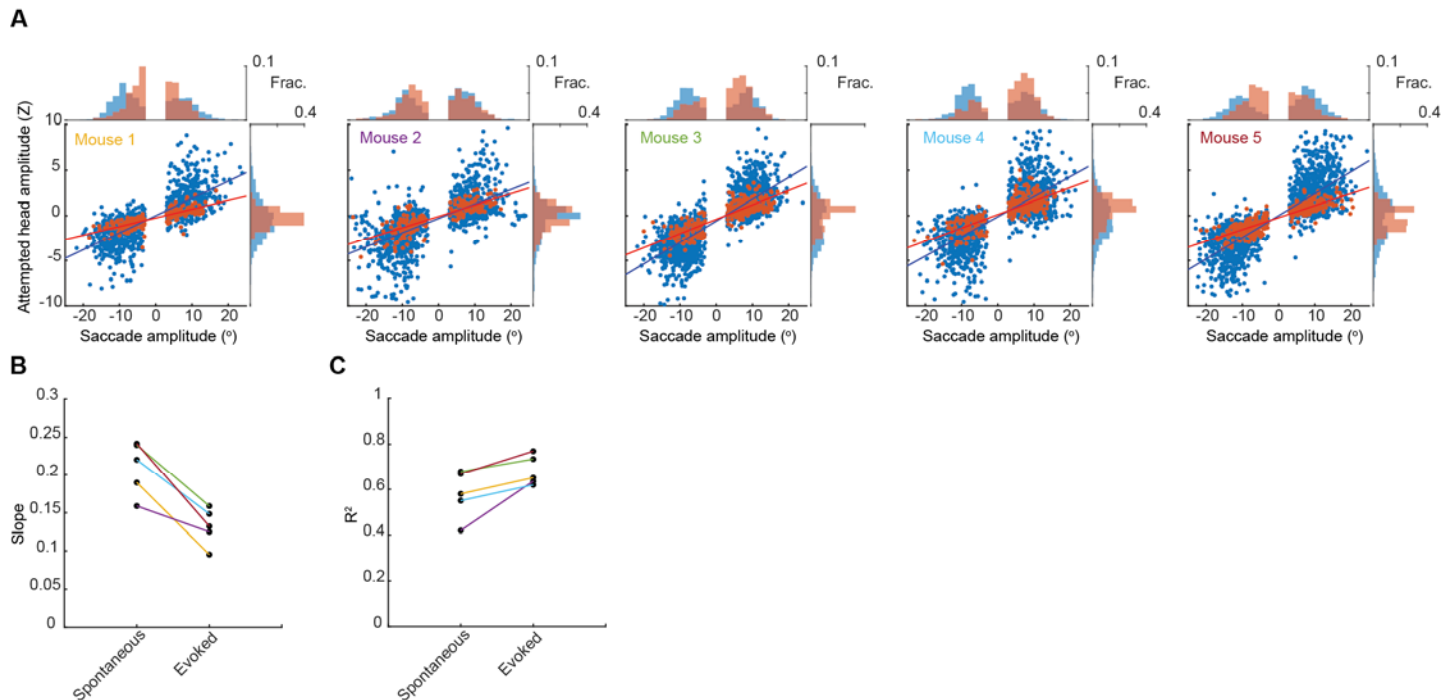
2   **Supplementary Figure 9. Gain of head-eye coupling variability across mice.** (A) Head-eye amplitude coupling of

3   spontaneous (blue) and ear airpuff-evoked saccades (red) for five individual mice. Each dot corresponds to a single

4   gaze shift. The spontaneous and evoked regression slopes were significantly different for all mice ($p < 10^{-5}$,

5   permutation test). Histograms above and beside scatter plot indicate distributions of saccade and attempted head

6   movement amplitudes.**(B, C)** Slope and R^2 for linear fits to spontaneous and evoked gaze shifts for each mouse.

7   Colored lines indicate values for the different mice in A.

8

1
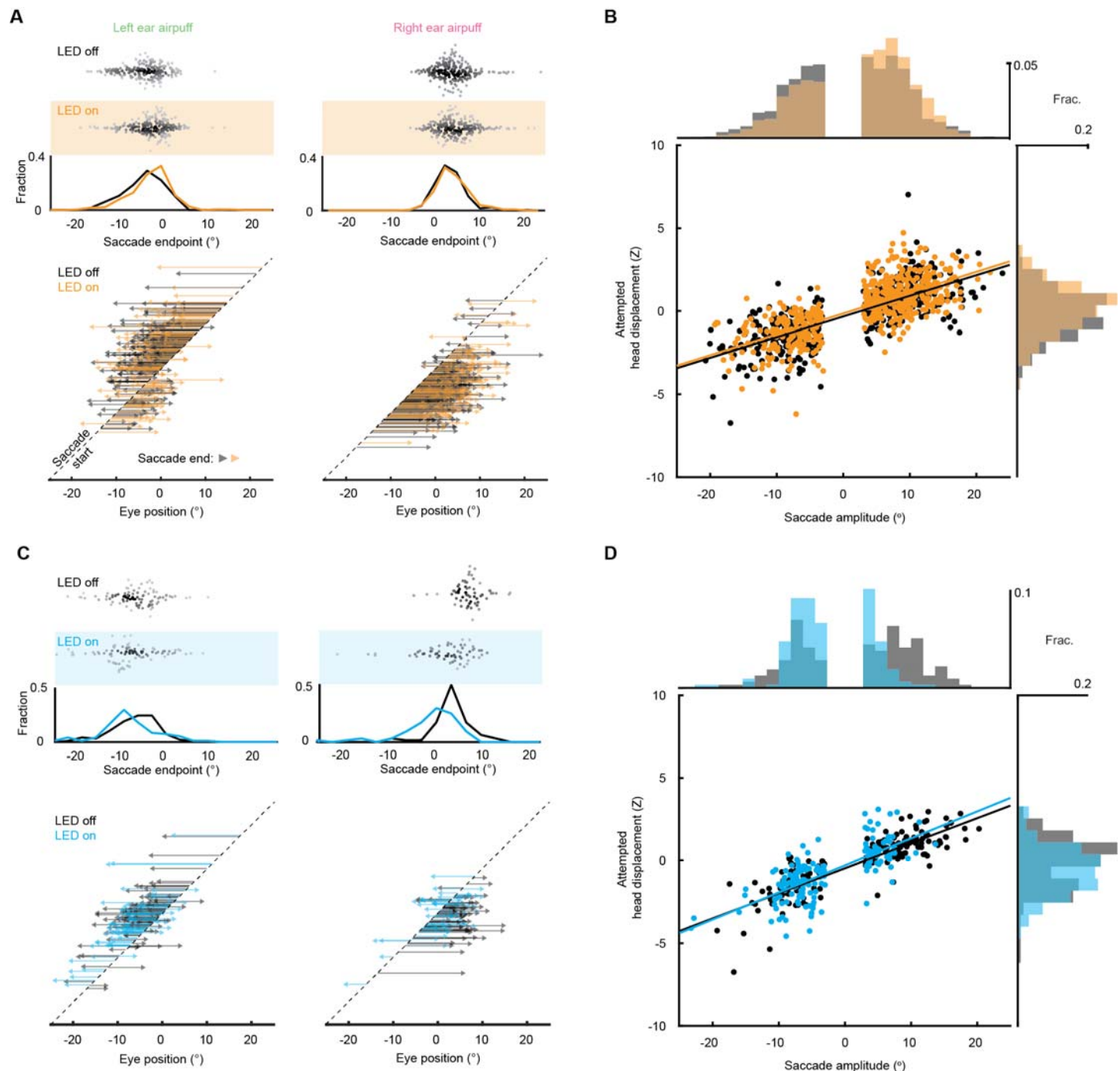
Supplementary Figure 10. **Controlling for the effects of initial eye position on superior colliculus**

manipulations. (A) Effects of SC optogenetic inhibition on saccade endpoints for trials matched for initial eye

position. Top, scatter plots and histograms of endpoints for control (white background) and LED on (orange

background) trials. Middle, endpoint histograms for control (black) and LED on (orange) trials. Bottom, saccade

vectors for control (black) and LED on (orange) trials. **(B)** Head-eye amplitude coupling during ear airpuff-evoked

1   gaze shifts for control (black) and LED on (orange) trials matched for initial eye position. Each dot represents an

2   individual gaze shift. Control: R^2 = 0.57, slope = 0.124, $p < 10^{-10}$. LED on: R^2 = 0.53, slope = 0.125, $p < 10^{-10}$. Control

3   and LED-on regression slopes were not significantly different (p = 0.41, permutation test) Histograms above and

4   beside scatter plot show distributions of saccade amplitude and head displacement, respectively. Distribution means

5   were significantly different (p = 0.002 for saccades, $p < 10^{-5}$ for attempted head movements, permutation test). **(C)**

6   Effects of weak SC optogenetic stimulation on saccade endpoints for trials matched for initial eye position. Top,

7   scatter plots and histograms of endpoints for control (white background) and LED on (blue background) trials. Middle,

8   histograms of endpoints for control (black) and LED on (blue) trials. Bottom, saccade vectors for control (black) and

9   LED on (blue) trials. **(D)** Head-eye amplitude coupling during ear airpuff-evoked gaze shifts for control (black) and

10   LED on (blue) trials matched for initial eye position. Each dot represents an individual gaze shift. Control: R^2 = 0.74,

11   slope = 0.15, $p < 10^{-10}$. LED on: R^2 = 0.52, slope = 0.164, $p < 10^{-10}$. Control and LED-on regression slopes were not

12   significantly different (p = 0.35, permutation test) Histograms above and beside scatter plot show distributions of

13   saccade amplitude and head displacement, respectively. Means were significantly different ($p < 10^{-5}$ for saccades, p

14   = 0.002 for attempted head movements, permutation test).

15

48

1   **Materials and Methods**

2   Mice: All experiments were performed according to Institutional Animal Care and Use

3   Committee standard procedures. C57BL/6J wild-type (Jackson Laboratory, stock 000664) mice

4   between 2 and 6 months of age were used. Mice were housed in a vivarium with a reversed

5   12:12 h light:dark cycle and tested during the dark phase. No statistical methods were used to

6   predetermine sample size. Behavioral experiments were not performed blinded as the

7   experimental setup and analyses are automated.

8   Surgical procedures: Mice were administered carprofen (5 mg/kg) 30 minutes prior to surgery.

9   Anesthesia was induced with inhalation of 2.5% isoflurane and buprenorphine (1.5 mg/kg) was

10   administered at the onset of the procedure. Isoflurane (0.5-2.5% in oxygen, 1 L/min) was used

11   to maintain anesthesia and adjusted based on the mouse's breath and reflexes. For all surgical

12   procedures, the skin was removed from the top of the head and a custom titanium headplate

13   was cemented to the leveled skull (Metabond, Parkell) and further secured with dental cement

14   (Ortho-Jet powder, Lang Dental). Craniotomies were made using a 0.5 mm burr and viral

15   vectors were delivered using pulled glass pipettes coupled to a microsyringe pump (Micro4,

16   World Precision Instruments) on a stereotaxic frame (Model 940, Kopf Instruments). Following

17   surgery, mice were allowed to recover in their home cages for at least 1 week.

18   Viral injections and implants: Coordinates for SC injections were ML: 1.25 mm, AP: 0.7 mm

19   (relative to lambda), DV: -1.9 and -2.1 mm (100 nL/depth). Coordinates for SC implants were

20   ML: 1.25 mm, AP: 0.7 mm (relative to lambda), DV: -2.0 mm. Fiber optic cannulae were

21   constructed from ceramic ferrules (CFLC440-10, Thorlabs) and optical fiber (400 mm core, 0.39

22   NA, FT400UMT) using low-autofluorescence epoxy (F112, Eccobond).

23   Behavioral procedures: To characterize stimulus-evoked gaze shifts (figures 1, 2, 3 and related

24   supplements), data were collected from 5 mice over 53 days (maximum of 1

49

1   session/mouse/day). Session types were randomly interleaved to yield a total of 6 ear airpuff

2   sessions, 6 ear tactile sessions, 6 whisker airpuff sessions, 10 auditory airpuff sessions, and 5

3   visual sessions. During experiments, headplated mice were secured in a custom 3D-printed

4   mouse holder. Timing and synchronization of the behavior were controlled by a microcontroller

5   (Arduino MEGA 2560 Rev3, Arduino) receiving serial commands from custom Matlab scripts. All

6   behavioral and data acquisition timing information was recorded by a NI DAQ (USB-6001) for

7   post hoc alignment. All experiments were performed using awake mice. Left and right stimuli

8   were randomly selected and presented at intervals drawn from a 7-12 s uniform distribution.

9   Each session consisted of 350 stimulus presentations and lasted ~55 minutes. No training or

10   habituation was necessary.

11   Stimuli: Airpuff stimuli were generated using custom 3D-printed airpuff nozzles (1.5 mm wide,

12   10 mm long) connected to compressed air that was gated by a solenoid. 3D-printed nozzles

13   were used to standardize stimulus alignment across experimental setups but similar results

14   were obtained in preliminary experiments using a diverse array of nozzle designs. For whisker

15   airpuffs, the nozzles were spaced 24 mm apart and centered 10 mm beneath the mouse's left

16   and right whiskers. For ear airpuffs, the nozzles were directed toward the ears while maintaining

17   10 mm of separation between the nozzles and the mouse. For auditory-only airpuffs, the

18   nozzles were directed away from the mouse while maintaining the same azimuthal position as

19   the ear airpuffs. For tactile-only stimulation, the ears were deflected using a thin metal bar

20   coated in epoxy to soften its edges (7122A37, McMaster). A stepper motor (Trinamic,

21   QSH2818-32-07-006 and TMC2208) was programmed to sweep the bar downward against the

22   ear before sweeping back up. The stepper motor was sandwiched between rubber pads

23   (8514K61, McMaster) and elevated on rubber pedestals (20125K73, McMaster) to reduce any

24   sound due to vibration. For visual stimulation, white LEDs (COM-00531, Sparkfun) were

25   mounted 6 inches from the mouse at the same azimuthal position as the airpuff nozzles.

1   <u>Eye tracking:</u> The movements of both left and right eyes was monitored at 100 Hz using two

2   high-speed cameras (BFS-U3-28S5M-C, Flir) coupled to a 110 mm working distance 0.5X

3   telecentric lens (#67- 303, Edmund Optics). A bandpass filter (FB850-40, Thorlabs) was

4   attached to the lens to block visible illumination. Three IR LEDs (475-1200-ND, DigiKey) were

5   used to illuminate the eye and one was aligned to the camera's vertical axis to generate a

6   corneal reflection. Videos were processed post hoc using DeepLabCut, a machine learning

7   package for tracking pose with user-defined body parts (Mathis et al., 2018). Data in this paper

8   were analyzed using a network trained on 1000 frames of recorded behavior from 8 mice (125

9   frames per mouse). The network was trained to detect the left and right edges of the pupil and

10   the left and right edges of the corneal reflection. Frames with a DeepLabCut-calculated

11   likelihood of $P < 0.90$ were discarded from analyses. Angular eye position (E) was determined

12   using a previously described method developed for C57BL/6J mice (Sakatani and Isa, 2004).

13   <u>Attempted head rotation tracking:</u> Attempted head rotations were measured using a 3D-printed

14   custom headplate holder coupled to a load cell force sensor (Sparkfun, SEN-14727). Load cell

15   measurements (sampling frequency 80 Hz) were converted to analog signals and recorded

16   using a NI DAQ (sampling frequency 2000 Hz). The data were then low-pass filtered at 80 Hz

17   using a zero-phase second-order Butterworth filter and then downsampled to match the pupil

18   sampling rate.

19   <u>Optogenetics:</u> Optogenetic experiments were performed using the ear airpuff nozzles. Fiber

20   optic cables were coupled to implanted fibers and the junction was shielded with black heat

21   shrink. A 470 nm fiber-coupled LED (M470F3, Thorlabs) was used to excite ChR2-expressing

22   neurons, and a 545 nm fiber-coupled LED (UHP-T-SR, Prizmatix) was used to inhibit

23   eNpHR3.0-expressing neurons. Optogenetic excitation during WISLR sessions was delivered

24   on a random 50% of trials using 1 s of illumination centered around airpuff onset.

1   *SC inhibition:* For optogenetic inactivation of SC neurons, AAV1.hSyn.eNpHR3.0 was injected

2   into the right SC of 5 wild-type mice (0.6 AP, 1.1 ML, -2.1 and -1.9 DV; 100 nl per depth).

3   Experiments were performed 35-40 days post injection. LED power was 12 mW. Mice

4   underwent 5 sessions each.

5   *SC stimulation:* For subthreshold optogenetic stimulation of SC neurons,

6   AAV1.CaMKIIa.hChR2(H134R)-EYFP was injected into the right SC of 4 wild-type mice.

7   Experiments were performed 67-71 days post injection. LED power was individually set to an

8   intensity that did not consistently evoke saccades upon LED onset (50-120uW). Mice underwent

9   5 sessions each.

10   Histology: For histological confirmation of fiber placement and injection site, mice were perfused

11   with PBS followed by 4% PFA. Brains were removed and post-fixed overnight in 4% PFA, and

12   stored in 20% sucrose solution for at least 1 day. Brains were sectioned at 50 µm thickness

13   using a cryostat (NX70, Cryostar), every third section was mounted, and slides were cover-

14   slipped using DAPI mounting medium (Southern Biotech). Tile scans were acquired using a

15   confocal microscope (LSM700, Zeiss) coupled to a 10X air objective.

16   Saccade detection: Saccades were defined as eye movements that exceeded 100°/s, were at

17   least 3° in amplitude, and were not preceded by a saccade in the previous 100 ms. The initial

18   positions and endpoints of saccades were defined as the first points at which saccade velocity

19   rose above 30°/s and fell below 20°/s, respectively. Analyses focused on horizontal saccades

20   because saccades were strongly confined to the azimuthal axis (Supplementary Fig. 1).

21   Behavioral analysis: Eye position analyses were performed using the averaged left and right

22   pupil positions, and the mean eye position was subtracted from each session prior to combining

23   data across sessions and mice. Similarly, attempted head rotation data was Z-scored prior to

24   combining data across sessions and mice. To quantify stimulus-evoked saccade probability, we

1   calculated the fraction of trials in which a saccade occurred in the 100 ms period following

2   stimulus onset (i.e. the response window). To quantify stimulus-evoked attempted head rotation

3   probability in Figure 1, we calculated the fraction of trials in which the Z-scored head sensor

4   reading exceeded 0.25Z 150 ms following stimulus onset. To determine the baseline head

5   movement probability, we calculated the fraction of trials in which the head sensor reading

6   exceeded 0.25Z between -500 ms and -350 ms relative to saccade onset.

7   To examine saccade endpoints, we first identified trials in which mice maintained fixation in the

8   500 ms preceding saccade onset. We then considered stimulus-evoked saccades those

9   occuring within 100 ms of stimulus onset.

10   To examine attempted head movement latencies, we first identified trials in which the mice

11   maintained head fixation from -1 to -0.5 s prior to saccade onset and used this period as the

12   baseline. Latency was defined as the first frame between -0.5 and 0.5 s relative to saccade

13   onset when the attempted head movement amplitude exceeded 5 standard deviations from that

14   trial's baseline.

15   To examine head-eye amplitude coupling during spontaneous and stimulus-evoked gaze shifts,

16   we identified trials in which the mouse maintained fixation in the 500 ms preceding saccade

17   onset. We defined attempted head rotation amplitude as the load cell value 150 ms following

18   saccade onset (the time point at which average load cell value plateaus during stimulus-evoked

19   gaze shifts (Fig. 3)). For certain analyses, we identified saccades matched (without

20   replacement) for initial eye position and/or saccade amplitude using Euclidean distance as a

21   metric and a 3° distance cutoff.

22   Tests for statistical significance are described in the text and figure legends. Data were shuffled

23   10,000 times to generate a null distribution for permutation tests.